

# DESIGN OF FULL-STRENGTH FULL-DUCTILITY EXTENDED END-PLATE BEAM-TO-COLUMN JOINTS

Antonella B. Francavilla, Massimo Latour, Vincenzo Piluso and Gianvittorio Rizzano  
Department of Civil Engineering, University of Salerno

## ABSTRACT

The analysis and modelling of the ultimate behaviour of the beam-to-column connections is certainly one of the most studied topics in the field of steel structures. In particular, seismic design of steel frames is commonly carried out to assure the dissipation of the seismic input energy in the so-called "dissipative zones" which have to be properly detailed in order to assure wide and stable hysteresis loops. Once avoided the yielding of columns, beam-to-column joints play a role of paramount importance. In fact, beam-to-column joints can be designed either as Full Strength (FS) or Partial Strength (PS). In the first case, the seismic input energy is dissipated by means of plastic cyclic excursions of the beam ends. In the second case, dissipation requires the plastic engagement of ductile joint components.

This paper addresses the design criteria to be adopted to assure full-strength full-ductility behaviour of Unstiffened Extended End-Plate (U-EEP) beam-to-column joints. The validation of the design procedure is accomplished by three-dimensional finite element analyses with ABAQUS 6.13 software. Finally, in order to clarify the design procedure in detail, a worked numerical example concerning the design of an external joint is presented.

## 1. INTRODUCTION

Within the analysis of steel structures, the modelling of the ultimate behaviour of beam-to-column joints is one of the most studied topic. As well known, before the introduction of the *semi-rigidity* concept [1,2], steel frame design was accomplished by properly considering a limit assumption regarding the joint behaviour. Depending on the beam-to-column joint typology, it was either assumed that all the ends of the members converging in the joint are subjected to the same rotation and the same displacements or assumed that the joints are able to permit free rotations. The first case leads to *continuous frames*, while the second one to *pinned frames*. The application of the semi-rigidity concept has required the development of a general methodology working out in detail the provision of the rotational stiffness and the flexural

30 resistance of joints. This resulted in a strong effort, in Europe more than in United States, which  
 31 has led to the complete definition and codification of the component method [3,4]. This allows  
 32 the analysis of actual semi-continuous structural systems, starting from the geometrical and  
 33 mechanical properties of beam-to-column joints.

34 The component method is essentially based on mechanical models constituted by the  
 35 assembling of spring elements modelling the joint components. The non-linearity of the joint  
 36 moment-rotation response is obtained starting from the inelastic constitutive laws adopted for  
 37 the components. The method is suitable for the modelling of any kind of joint provided that the  
 38 components are properly identified and their constitutive law is deservedly modelled.

39 Even though some authors have already investigated some aspects related to the prediction  
 40 of the plastic deformation capacity [5-8, 39, 40] and of the cyclic behaviour of connections [9-  
 41 13, 41] past experimental and theoretical researches have often focused their attention mainly  
 42 on the prediction of the stiffness and resistance of joint components. Therefore, the prediction  
 43 of the plastic deformation capacity of connections is still an open research field whose primary  
 44 aim is devoted to the prediction of the plastic rotation capacity of partial strength connections.

45 Moreover, it cannot be denied that the classification of beam-to-column joints as full-  
 46 strength or as partial-strength is too simplistic, because it is rigorous only in the pure  
 47 theoretical case in which both the joint that the connected member exhibit a perfectly plastic  
 48 behaviour. As soon as the distinction between the joint and the connection is made (Fig.1),  
 49 allowing the definition of the joint as the combination in series of the connection and the panel  
 50 zone of the column web, also the concept of **beam-joint system** becomes noticeable, being  
 51 constituted by the combination in series of the beam-to-column joint and the beam end [14].

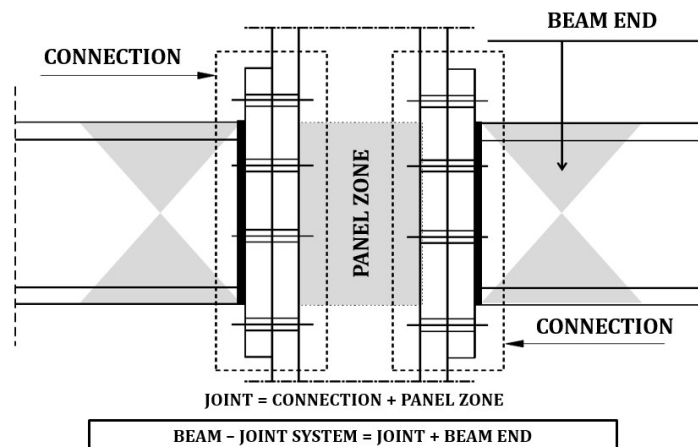


**Figure 1 - Beam-joint system**

52 This concept is of primary importance under the point of view of yielding location and,  
 53 therefore, for seismic design purposes. This statement can be easily explained considering a tri-  
 54 linear modelling of the moment-rotation curve of both the beam-to-column joint and the beam  
 55 end (Fig.2). In fact, generally the plastic rotation supply  $\Theta_{pu}$  of the beam-joint system can be  
 56 regarded as the sum of two contributions: the plastic rotation of the beam-to-column joint  $\varphi_p$   
 57 and the plastic rotation provided by the beam end  $\vartheta_p$ . Therefore, an accurate evaluation of the  
 58 moment-rotation curve of the beam-to-column joint is required, because the plastic rotation  
 59 provided by the beam end is strictly dependent on the flexural resistance that the beam-to-  
 60 column joint is able to develop [14].

61 Concerning beam-to-column joint,  $M_{j,y}$  is the value of the bending moment leading to first  
 62 yielding,  $M_{j,p}$  is the conventional plastic moment defining the knee of the moment-rotation  
 63 curve according to Eurocode 3,  $M_{j,u}$  is the theoretical ultimate flexural resistance of the beam-  
 64 to-column joint. Regarding the beam,  $s M_{pb}$  is the bending moment corresponding to the  
 65 occurrence of local buckling of the beam compressed flange.

66 The parameter  $s$  is the non-dimensional buckling stress depending on the width-to-thickness  
 67 ratios of the plate elements constituting the beam section and on the longitudinal stress  
 68 gradient. Starting from the analysis of the experimental data [15,16], by means of a multiple  
 69 regression analysis, Mazzolani and Piluso [17] defined the following empirical relationship:

$$s = \frac{1}{0.546321 + 1.632533\lambda_f^2 + 0.062124\lambda_w^2 - 0.602125\frac{b_f}{L_e} + 0.001471\frac{E}{E_h} + 0.007766\frac{\varepsilon_h}{\varepsilon_y}} \leq \frac{f_u}{f_y} \quad (1)$$

70 where  $\lambda_f$  and  $\lambda_w$  are, respectively, the normalized slenderness parameters of the flange and of  
 71 the web equal to:

$$\lambda_f = \frac{b_f}{2 t_f} \sqrt{\frac{f_{ym.bf}}{E}} \quad \text{and} \quad \lambda_w = \frac{d_w}{2 t_w} \sqrt{\frac{f_{ym.bw}}{E}} \quad (2)$$

72 where  $b_f$  is the flange width,  $t_f$  is the flange thickness,  $d_w$  is the compressed part of the beam  
 73 web,  $t_w$  is the web thickness,  $L_e$  is the shear length of the beam,  $E$  is the Young modulus,  $f_{ym.bf}$  is  
 74 the average value of the yielding resistance of the beam flange,  $f_{ym.bw}$  is the average value of the  
 75 yielding resistance of the beam web,  $E_h$  is the hardening modulus,  $\varepsilon_y$  is the strain corresponding  
 76 to yielding,  $\varepsilon_h$  is the strain corresponding to the end of the yield plateau and  $f_u$  and  $f_y$  are  
 77 respectively the ultimate and the yielding resistance of the material composing the beam.

78 Four significant cases can arise [14] (Fig.2):

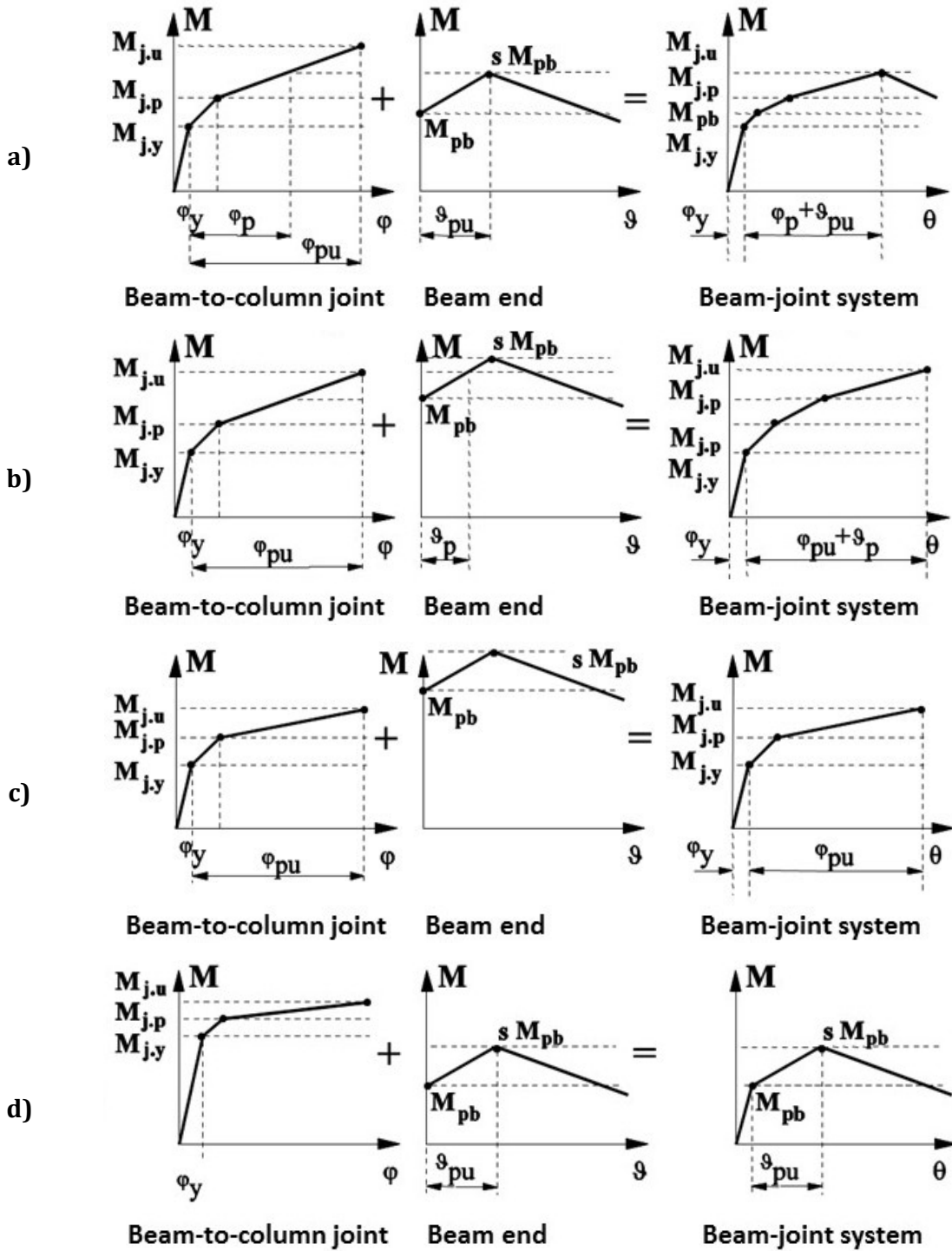


Figure 2 - Plastic rotation supply of the beam-joint system [14]

79

80 a)  $M_{j,u} \geq s M_{pb}$

81 In this case the ultimate resistance of the beam-to-column joint allows the complete

82 exploitation of the beam plastic reserves, so that:

$$\vartheta_p = \vartheta_{pu} \quad \text{and} \quad \varphi_p \leq \varphi_{pu} \quad (3)$$

83 where  $\vartheta_{pu}$  is the ultimate plastic rotation of the beam and  $\varphi_{pu}$  is the theoretical value of the  
84 ultimate plastic rotation of the beam-to-column joint.

85 Therefore, the plastic rotation supply of the beam-joint system is given by the sum of the  
86 beam plastic rotation supply and a part, for  $M_{j.u} > s M_{pb}$ , or the total value, for  $M_{j.u} =$   
87  $s M_{pb}$ , of the plastic rotation supply of the beam-to-column joint. As the plastic rotation  
88 supply of the beam-joint system is greater than the plastic rotation capacity of the connected  
89 beam, the beam-to-column joints can be defined as full-strength full-ductility.

90 b)  $M_{pb} \leq M_{j.u} < s M_{pb}$

91 In this case, even though the beam end can be engaged in plastic range, the ultimate  
92 resistance of the beam-to-column joint is not sufficient to completely exploit the beam  
93 plastic reserves, so that:

$$\vartheta_p < \vartheta_{pu} \quad \text{and} \quad \varphi_p = \varphi_{pu} \quad (4)$$

94 Therefore, the plastic rotation supply of the beam-joint system is given by the sum of the  
95 plastic rotation supply of the joint and of a part of that of the connected beam. The beam-to-  
96 column joint can be defined as full-strength (because  $M_{j.u} > M_{pb}$ ), but cannot be defined “a  
97 priori” as full-ductility, because the plastic rotation capacity of the beam-joint system is  
98 strictly dependent on the contribution ( $\varphi_{pu}$ ) due to the beam-to-column joint.

99 c)  $M_{j.u} \leq M_{pb}$

100 In this case, the ultimate resistance of the beam-to-column joint is not sufficient to engage  
101 the beam in plastic range, so that:

$$\vartheta_p = 0 \quad \text{and} \quad \varphi_p = \varphi_{pu} \quad (5)$$

102 Therefore, the ultimate plastic rotation of the beam-joint system is coincident with the  
103 plastic rotation of the beam-to-column joint. The beam-to-column joint can be defined as  
104 partial-strength. Nothing can be said, a priori, about on the degree of restoration of rotation  
105 capacity, because the plastic rotation capacity of the beam-joint system is strictly dependent  
106 on  $\varphi_{pu}$ .

107 d)  $M_{j.y} > s M_{pb}$

108 In this case, the elastic flexural resistance is sufficient to completely exploit the plastic  
109 reserves of the beam, so that:

$$\vartheta_p = \vartheta_{pu} \quad \text{and} \quad \varphi_p = 0 \quad (6)$$

110 Consequently, the plastic rotation of the beam-joint system is equal to the plastic rotation  
111 of the beam end. The beam-to-column joint can be referred as full-strength full-ductility.  
112 The difference with respect to case a) is that the beam-to-column joint remains in elastic  
113 range ( $\varphi_p = 0$ ).

114 Regarding the evaluation of the plastic rotation of the beam end, simple relations are  
115 available in literature [18-21]. In addition, the plastic rotation of the beam-to-column joints can  
116 be determined starting to the knowledge of the plastic deformation of each component, through  
117 an advanced modelling of their force-displacement law (up to the ultimate displacement). In  
118 fact, the plastic displacement occurring at the tensile flange level is equal to the sum of the  
119 ultimate displacement of the weakest component and of the contributions of the other  
120 components. The resulting plastic rotation is given by the ratio of that such plastic displacement  
121 and the level arm [14].

122 It is important to underline that the above classification approach of the beam-to-column  
123 connection as full-strength or as partial strength is different from that adopted in Eurocodes.  
124 In Eurocode 3 Part 1-8 [3], it is clearly stated that a joint can be classified as full-strength by  
125 comparing its design moment resistance  $M_{j,Rd}$  with the design moment resistance of the  
126 connected member  $M_{b,Rd}$ . Conversely, as the classification approach herein presented is mainly  
127 devoted to underline the role of the joint flexural resistance on the plastic rotation supply of  
128 the beam-joint system, the comparison is based on the ultimate bending moment. Therefore, it  
129 is useful to keep in mind that having  $M_{j,Rd} \geq s M_{b,Rd}$  does not necessarily mean that  $M_{j,Rd} \geq$   
130  $M_{b,Rd}$ . However, as previously mentioned, the classification adopted by Eurocode 3 is rigorous  
131 only in the pure theoretical case occurring when both the joint and the connected member  
132 exhibit a perfectly plastic behaviour.

133

## 134 **2. CAPACITY DESIGN OF BEAM-TO-COLUMN JOINTS**

135 The design of beam-to-column joints is traditionally aimed to assure that yielding occurs at  
136 the beam ends of the connected beam where the dissipation of the earthquake input energy is  
137 expected relying on wide and stable hysteresis loops. To this aim, Eurocode 8 [22] requires that  
138 the degree of overstrength required is guaranteed in case of full penetration butt welds or  
139 satisfying, in case of other joint typologies, the following relationship:

$$M_{j.Rd} > 1.1 \cdot \gamma_{ov} \cdot M_{b.Rd} \quad (7)$$

140 where  $M_{j.Rd}$  represents the joint design resistance,  $M_{b.Rd}$  the plastic moment of the connected  
 141 beam and  $\gamma_{ov}$  is an overstrength factor accounting for the random variability of the steel yield  
 142 strength, while the coefficient 1.1 covers the effects of material strain hardening. Eurocode 8  
 143 recommends the use of  $\gamma_{ov} = 1.25$ ; conversely, the Italian code [23] suggests a joint  
 144 overstrength coefficient depending on the steel grade ( $\gamma_{ov} = 1.20$  for S235,  $\gamma_{ov} = 1.15$  for S275  
 145 and  $\gamma_{ov} = 1.10$  for S355).

146 One of the causes of significant and premature joint damage during the seismic events of  
 147 Northridge and Kobe can be recognised in the use of design criteria not able to assure a  
 148 sufficient degree of overstrength to allow the full development of the beam plastic rotation  
 149 capacity. In fact, regarding the overstrength which the beam is able to exhibit, due to strain  
 150 hardening, it depends on the width-to-thickness ratios of flanges and web. As a consequence,  
 151 the joint overstrength needed to assure the full-strength requirement is strictly related to the  
 152 behavioural class of the beam section (i.e. ductile, compact, semi-compact and slender). It  
 153 means that, decreasing the width-to-thickness ratios of flanges and web, the plastic  
 154 deformation capacity of the beam increases, but this beneficial effect could be vanished if the  
 155 beam-to-column joint does not possess the overstrength required by the simultaneous increase  
 156 of the beam ultimate resistance. In addition, also the influence of random material variability  
 157 both on the beam flexural resistance and the beam-to-column joint moment resistance has to  
 158 be properly accounted for.

159 Only a few studies concerning the influence of random material variability on the behaviour  
 160 of steel connections are available [24-27]. In particular, it has been proposed [24] to formulate  
 161 the design requirement for full-strength and full-ductility joints by means of a probabilistic  
 162 approach calibrated on the basis of the results coming from Monte Carlo simulations [28],  
 163 including both the random material variability of the plate elements and that of bolt properties  
 164 [29].

165 A simplified approach to account for the influence of random material variability is herein  
 166 proposed by assuming an overstrength factor  $\gamma_{ov,rm}$  equal to the ratio between the average  
 167 value of the yield strength of beam flanges  $f_{ym,bf}$  and the nominal yield strength  $f_{y,b}$ .  
 168 Conversely, the amount of overstrength due to the development of strain-hardening up to the  
 169 occurrence of local buckling is taken into account directly considering the width-to-thickness  
 170 ratios of beam flanges and web. Therefore, the ultimate beam flexural resistance at the plastic  
 171 hinge location is evaluated as:

$$M_{b,u} = \gamma_{ov.rm} \cdot \gamma_{ov.sh} \cdot \gamma_{M0} \cdot M_{b,p} \quad (8)$$

172 where:

$$M_{b,p} = \frac{Z_b \cdot f_{y,b}}{\gamma_{M0}} \quad (9)$$

173 being  $Z_b$  the plastic modulus of the beam section,  $f_{y,b}$  is the yielding resistance of the beam and  
 174  $\gamma_{M0}$  the partial safety factor.

175 The average yield strength of beam flanges is evaluated accounting for the influence of the  
 176 flange thickness  $t_{bf}$ , so that:

$$\gamma_{ov.rm} = \frac{f_{ym,bf}}{f_{y,b}} = \frac{f_0 - \beta t_{bf}}{f_{y,b}} \quad (10)$$

177

178 where the parameters  $f_0$  and  $\beta$  depend on the steel grade (Table 1).

179 The coefficient  $\gamma_{ov.sh}$  accounting for the influence of strain hardening is given by  
 180  $\gamma_{ov.sh} = s$  [17], where  $s$  is the parameter given by Eq. (1).

181

**Table 1:** Mechanical properties of the material

Steel classes	$f_0$ [MPa]	$\beta$ [MPa/mm]	$\frac{E}{E_h}$	$\frac{\epsilon_h}{\epsilon_y}$
S 235	313.4	2.254	37.5	12.3
S 275	323.3	0.910	42.8	11.0
S 355	444.2	2.987	48.2	9.8

182

### 183 3. DESIGN PROCEDURE FOR FULL-STRENGTH FULL-DUCTILITY 184 JOINTS

185 Starting from the average ultimate resistance of the beam provided by Eq. (8), a design  
 186 procedure aiming to the development of full-strength full-ductility joints is proposed and  
 187 discussed with reference to extended end-plate joints with four bolts in tension. The end-plate  
 188 is unstiffened. The design goal is accomplished by properly applying the basic principles of  
 189 "capacity design" at component level, considering all the joint components defined by Eurocode  
 190 3 within the framework of the "component method".



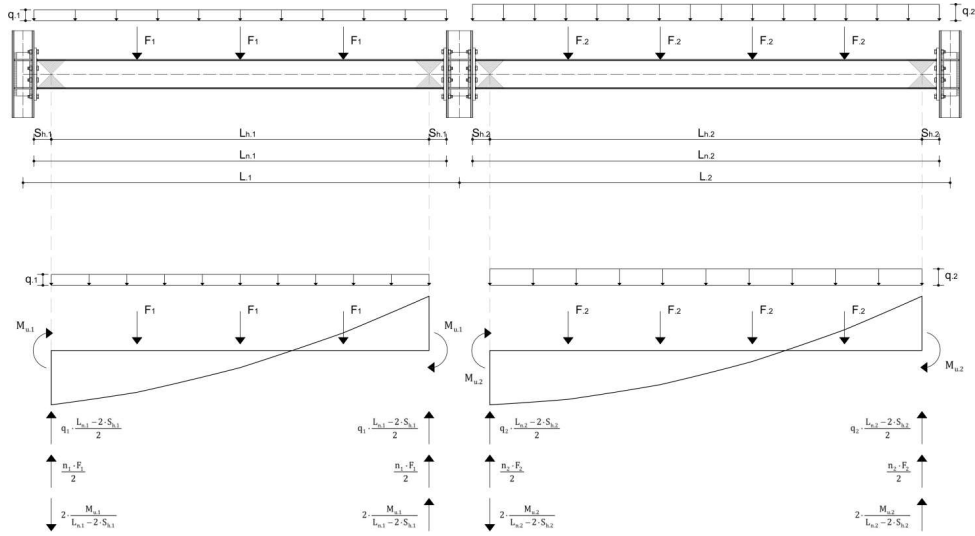


**Figure 3** - Reference structural scheme considering seismic actions from left to right

191

192 In particular, the proposed procedure starts from the identification of the maximum internal  
 193 actions which the fully yielded and strain-hardened beam is able to transmit to the joint. The  
 194 reference structural scheme is depicted in Fig. 3. By denoting with  $i$  the left end joint and with  $j$   
 195 the right end joint for each beam and considering seismic actions from left to right, the shear  
 196 action occurring at the plastic hinge locations are given by:

$$\begin{aligned}
 V_{bu.i}^{(1)} &= \frac{q_1 L_{h1}}{2} + \frac{n_{F1} F_1}{2} - \frac{2 M_{bu.1}}{L_{h1}} & V_{bu.j}^{(1)} &= \frac{q_1 L_{h1}}{2} + \frac{n_{F1} F_1}{2} + \frac{2 M_{bu.1}}{L_{h1}} \\
 V_{bu.i}^{(2)} &= \frac{q_2 L_{h2}}{2} + \frac{n_{F2} F_2}{2} - \frac{2 M_{bu.2}}{L_{h2}} & V_{bu.j}^{(2)} &= \frac{q_2 L_{h2}}{2} + \frac{n_{F2} F_2}{2} + \frac{2 M_{bu.2}}{L_{h2}}
 \end{aligned} \tag{11}$$

197

198 where the vertical loads  $q$  are those occurring in the seismic load combination ( $G_k + \psi_2 Q_k$ )  
 199 according to Eurocode 8,  $L_h$  is the distance between the two plastic hinges,  $F$  are the  
 200 concentrated forces due to the secondary beams applied symmetrically according to the beam  
 201 centre and  $n_F$  is the number of these forces. The parameter  $s_h$ , i.e. the distance between the  
 202 plastic hinge and the column flange, is taken equal to the beam height.

203 On the basis of the maximum moment which the beams are able to transmit given by Eq. (8),  
 204 the bending moment  $M_{cf}$  and shear action  $V_{cf}$  at the column flange can be evaluated as follows:

205 a) in the case of external joint  $i$  of beam 1:

$$M_{cf.i}^{(1)} = M_{bu.1} - V_{bu.i}^{(1)} \cdot s_{h1} - \frac{q_1 s_{h1}^2}{2} \quad V_{cf.i}^{(1)} = V_{bu.i}^{(1)} + q_1 s_{h1} \tag{12}$$

206 b) in the case of internal joint  $j$  of beam 1:

$$M_{cf.j}^{(1)} = M_{bu.1} + V_{bu.i}^{(1)} \cdot s_{h1} + \frac{q_1 s_{h1}^2}{2} \quad V_{cf.j}^{(1)} = V_{bu.j}^{(1)} + q_1 s_{h1} \quad (13)$$

207 c) in the case of internal joint i of beam 2:

$$M_{cf.i}^{(2)} = M_{bu.2} - V_{bu.i}^{(2)} \cdot s_{h2} - \frac{q_2 s_{h2}^2}{2} \quad V_{cf.i}^{(2)} = V_{bu.i}^{(2)} + q_2 s_{h2} \quad (14)$$

208 d) in the case of external joint j of beam 2:

$$M_{cf.j}^{(2)} = M_{bu.2} + V_{bu.i}^{(2)} \cdot s_{h2} + \frac{q_2 s_{h2}^2}{2} \quad V_{cf.j}^{(2)} = V_{bu.j}^{(2)} + q_2 s_{h2} \quad (15)$$

209 Obviously, the analysis is repeated for the case of seismic actions from left to right and the  
210 most severe internal actions are considered.

211 Regarding the design of column web panel stiffeners, they have to be designed considering  
212 the maximum shear action occurring when the beams are in the ultimate conditions and the  
213 shear action acting in the columns  $V_c$ .

214 e) In the case of panel zone of external joint i of first bay:

$$V_{wp.Ed} = \frac{M_{cf.i}^{(1)}}{d_{b1} - t_{bf.1}} - \frac{V_{c1} + V_{c2}}{2} \quad (16)$$

215 f) In the case of panel zone of internal joint:

$$V_{wp.Ed} = \frac{M_{cf.j}^{(1)}}{d_{b1} - t_{bf.1}} + \frac{M_{cf.i}^{(2)}}{d_{b2} - t_{bf.2}} - \frac{V_{c1} + V_{c2}}{2} \quad (17)$$

216 g) For the external panel zone j of the beam 2:

$$V_{wp.Ed} = \frac{M_{cf.j}^{(2)}}{d_{b2} - t_{bf.2}} - \frac{V_{c1} + V_{c2}}{2} \quad (18)$$

217 In the case of extended end plate connections with four bolts in tension, according to  
218 Eurocode 3, a simplified model can be adopted to design the tension zone by means on an  
219 equivalent T-stub whose lever arm is equal to  $d_b - t_{bf}$  (Fig. 4). However, according to Eurocode 3,  
220 when the this model is adopted as a conservative simplification, also a ductility criterion has to  
221 be adopted. Such criterion requires that the total design resistance  $F_{Rd}$  shall not exceed  
222  $3.8 F_{t,Rd}$ , where  $F_{t,Rd}$  is the design tension resistance of a bolt. Notwithstanding this criterion  
223 has been herein neglected, because sufficient bolt overstrength is already guaranteed by means  
224 of the use of hierarchy criteria. In fact, Eurocode 3 requirement concerning the use of the  
225 simplified T-stub model corresponds to a bolt overstrength of about 5% (i.e.  $4/3.8=1.05$ ). This  
226 bolt overstrength is surely guaranteed when hierarchy criteria for seismic design are applied  
227 because the overstrength coefficient  $\gamma_{ov.sh}$  is always  $> 1.05$ .

228 According to this model, the design of all the joint components has to guarantee the  
 229 transmission, at the beam flanges' levels, of a compression force  $C_u$  and of a tensile force  $T_u$   
 230 given by:

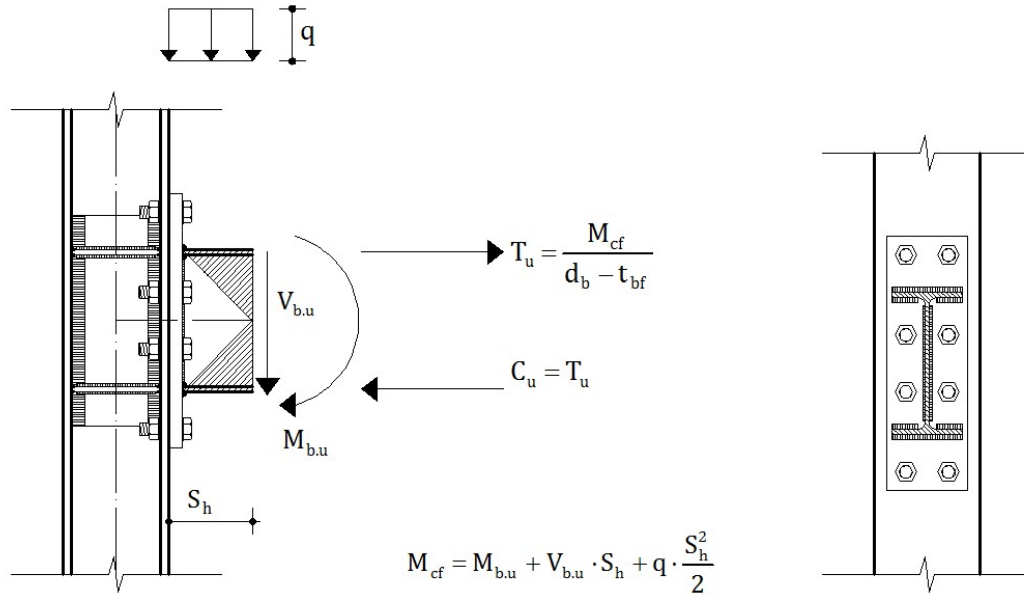


**Figure 4:** Simplified model for the design of the tension zone

231

$$T_u = C_u = \frac{M_{cf}}{d_b - t_{bf}} \quad (19)$$

232 Starting from the knowledge of  $T_u$  and  $C_u$  values occurring when the beam plastic hinges have  
 233 attained their ultimate flexural resistance, all the geometrical details of the connecting elements  
 234 can be designed by means of the resistance formulations provided by Eurocode 3 for the joint  
 235 components. To this aim, a specific sequence of design operations or resistance checks of the  
 236 joint components has to be followed:

237 **Step 1:** Evaluation, by means of Eq. (8), of the average (because of random material variability)  
 238 ultimate moment  $M_{b,u}$  which the fully yielded and strain-hardened beam is able to  
 239 transmit.

240 **Step 2:** Calculation of bending moment  $M_{cf}$  and shear action  $V_{cf}$  at the column flange and  
 241 evaluation of compression force  $C_u$  and tensile force  $T_u$  to be transmitted at the beam  
 242 flanges' levels.

243 **Step 3:** Design of the bolt diameter accounting for the combined action of shear and tension.

244 **Step 4:** Design of throat thickness of welds connecting the end-plate to the beam flange and  
 245 design of throat thickness of welds connecting the end-plate to the beam web assuming

246 that they have to transmit a bending moment proportional to the plastic modulus of the  
247 beam web alone.

248 **Step 5:** Design of the end-plate thickness by modelling the tension zone by means of an  
249 equivalent T-stub and assuming that the distance  $m$  between the bolt axis and the yield  
250 line located close to the beam flange is equal to the minimum allowed by the code,  $m=1.2$   
251  $d_o$  with  $d_o$  equal to the diameter of the hole; the width of the end-plate can be defined  
252 considering code requirements concerning the bolt spacing and the edge distances.

253 **Step 6:** Check of the resistance of the column web in shear and design of supplementary web  
254 plates if needed. Eurocode 3 introduces a limitation about the thickness of the  
255 supplementary plates. In particular, the shear area  $A_{vc}$  may be increased no more than  
256  $b_{stwc}$ . If a further supplementary web plate is added on the other side of the web, no  
257 further increase of the shear area is allowed. The proposed method does not take into  
258 account such limitation.

259 **Step 7:** Check of the resistance of the column web in tension and in compression; if needed  
260 continuity plates are added and/or supplementary web plates are extended to cover also  
261 tension and compression zones.

262 **Step 8:** Check of the resistance of the column flange in bending; if not satisfied, backing plates  
263 can be adopted to increase the resistance of the equivalent T-stub modelling the column  
264 flange in bending. It should be underlined that the adoption of the backing plates is  
265 useful when type 1 mechanism occurs, otherwise (type 2 mechanism) the increase of the  
266 bolt diameter is needed and the procedure has to be repeated starting from step 3.

## 267 **4. DESIGN EXAMPLES AND FINITE ELEMENT MODELLING**

268 Reference is made to the layout depicted in Fig. 5.

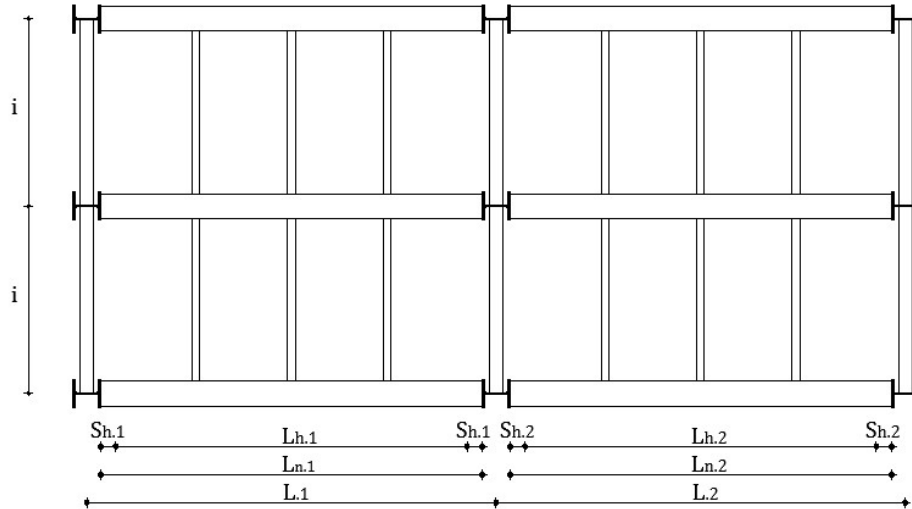


**Figure 5:** Building plan layout of study cases

269

270

271

272

Three different solutions have been designed with reference to the external joint of the longitudinal inner frame by varying the geometry of the structure. In Table 2, the input data for the three cases analysed are summarized.

**Table 2 -** Input data of case studies

Study case	Beam section	Column section	Beam steel grade	Column steel grade	Plates steel grade	Bolt class	q [kN/m]	F [kN]	$n_F$	$L_n$ [mm]
A	IPE 600	HEM 320					1.25	65	3	8641
B	IPE 450	HEM 260	S235	S355	S275	10.9	1.00	45	3	6232
C	IPE 220	HEM 200					0.75	30	3	3800

273

274

275

276

277

278

279

280

281

282

For the sake of simplicity the detailed calculations are not reported here and the main results obtained both with the proposed and with the EC8 design procedures are directly summarized in Table 3. Nevertheless, in order to clarify the proposed design method one of the cases, namely the case A, is described in detail in a worked example reported in Annex. From Table 3 it can be observed that the most important difference occurs for the case study C, i.e. in the case with the smallest beam size, where the design bending moment according to the proposed design procedure is about the 36.4% greater than the one required according to Eurocode 8. This difference reduces to the 26.5% for study case B and to 23.6% for study case A. It is worth to observe that this difference, in two cases out of three, exceeds the value of the partial safety

283 factor  $\gamma_{M2}=1.25$  suggested by EC8 for the design of bolts and welds and, therefore, it is expected  
 284 that, in these cases, the EC8 design procedure may fail.

**Table 3 – Design solutions for analysed study cases**

Study case	Design procedure	$\gamma_{ov,rm}$	$\gamma_{ov,sh}$	$M_{cf}$ [kNm]	$V_{cf}$ [kN]	$T_u$ [kN]	$d_b$ [mm]	$a_f$ [mm]	$a_w$ [mm]	$t_{ep}$ [mm]	$t_s$ [mm]	$t_{cp}$ [mm]	$a_{cp}$ [mm]	$\frac{F_{Rd.1}}{T_u}$	$\frac{F_{Rd.2}}{T_u}$
A	Eurocode 8	1.25	1.10	1081	353	1860	33	23	10	45	-	20	8	3.56	1.39
	Proposal	1.15	1.28	1336	405	2299	36	29	10	55	5	20	8	2.79	1.18
B	Eurocode 8	1.25	1.10	524	239	1203	27	18	8	35	-	15	6	3.73	1.41
	Proposal	1.24	1.26	663	278	1524	30	22	9	45	5	15	6	2.94	1.22
C	Eurocode 8	1.25	1.10	88	93	417	16	11	5	20	-	10	4	2.29	1.08
	Proposal	1.25	1.30	120	107	571	20	14	6	25	5	10	4	1.67	1.03

285  
 286 In order to evaluate the accuracy of the examined design criteria, numerical simulations by  
 287 means of advanced finite element models have been performed using ABAQUS 6.13 software.  
 288 Since the behaviour of the analysed connections is strongly affected by in-plane and out-of-  
 289 plane deformations, by contacts between the connecting elements and the profiles of column  
 290 and beam and by geometrical and material non linearities, the finite element model has been  
 291 developed adopting a three-dimensional approach based on the following steps: geometrical  
 292 characterization of the components, definition of material properties, definition of the  
 293 interactions between the elements, definition of the boundary conditions and choice of the  
 294 elements and size of the mesh, calibration and application of a proper initial imperfection  
 295 model.

296 The simulation has been performed considering the scheme depicted in Fig. 6, restrained  
 297 with a hinge at the bottom end of the column and a roller at the top end of the column,  
 298 preventing horizontal displacements of the top column end. The beam end is loaded with a  
 299 vertical force inducing in the joint a combination of shear and bending consistent with the  
 300 actions arising in the reference scheme under seismic loads.

301 To this aim, the length of the beam has been assumed equal to  $M_{cf}/V_{cf}$ , thus assuring that  
 302 when the design bending resistance is attained also the corresponding shear action is achieved.  
 303 The length of the column has been assumed equal to 3500 mm, i.e. the interstorey height of the  
 304 sample building.

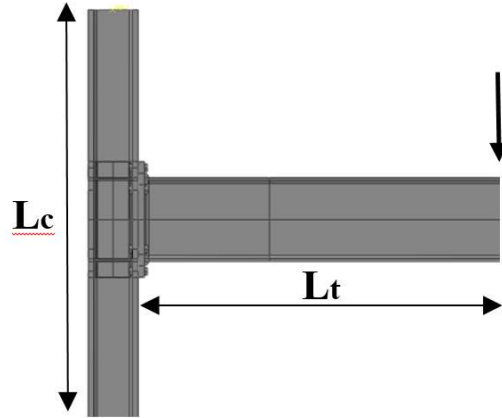


**Figure 6:** Analysed structural scheme

305

306 Regarding the *geometrical definition* of the components, the model is made up of seven  
 307 repetitive elements: the column, the beam, the end plate, the bolts, the continuity plates and the  
 308 additional supplementary web plates (Fig. 7).

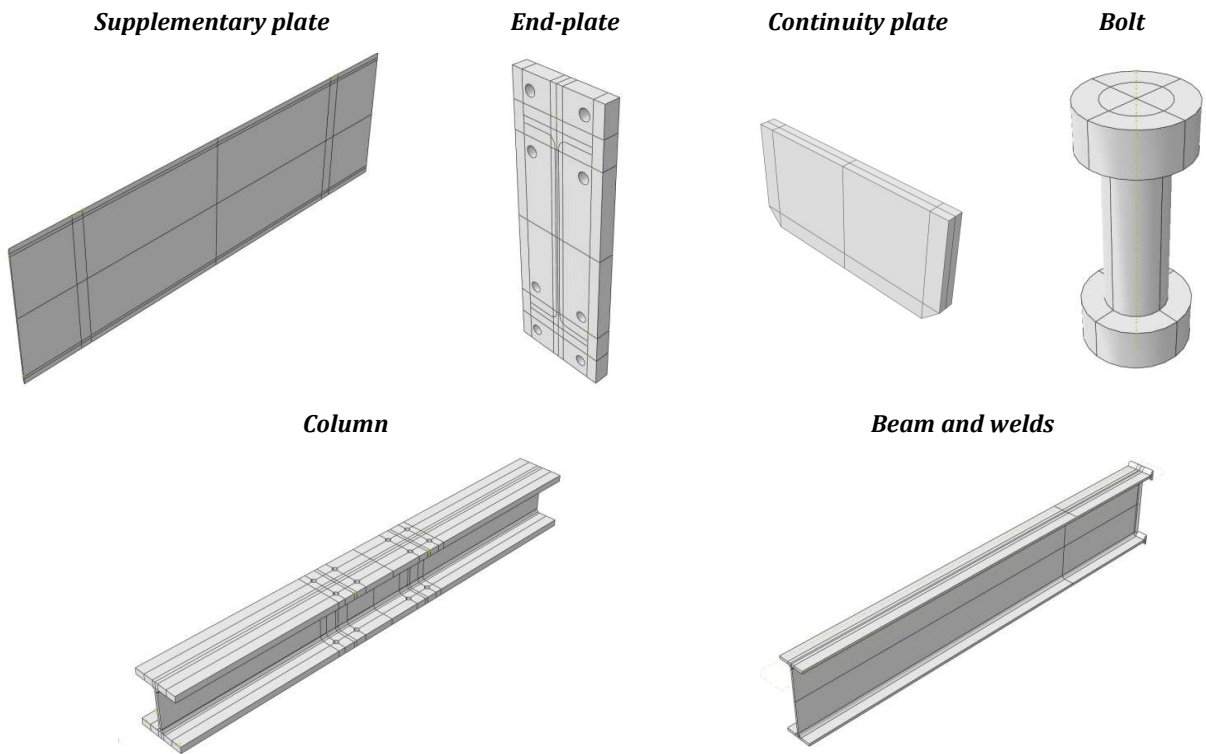


**Figure 7:** Components of the finite element model

309

310 The *material properties* of the plate elements and of the profiles have been described by  
 311 means of an elastic-plastic isotropic model by adopting a quadrilinear true stress-true strain  
 312 law (Fig. 8a). The parameters for different constructional steels are given in Table 2.

313 The behaviour of the material of the bolts has been modelled using a simplified tri-linear  
 314 model (Fig. 8b) based on the yield and ultimate nominal strength according to the bolt class.  
 315 The strain corresponding to the ultimate resistance and the ultimate strain have been evaluated  
 316 by means of the following relationships:  $\varepsilon_m = A_r [\%]$  and  $\varepsilon_u = \ln (1/1-Z)$ , where  $A_r$  is elongation  
 317 at fracture and  $Z$  is the necking ratio given by the ratio between the original cross-sectional area  
 318 and the minimum cross-sectional area after fracture. The values provided by the manufacturer  
 319 [30] have been adopted.

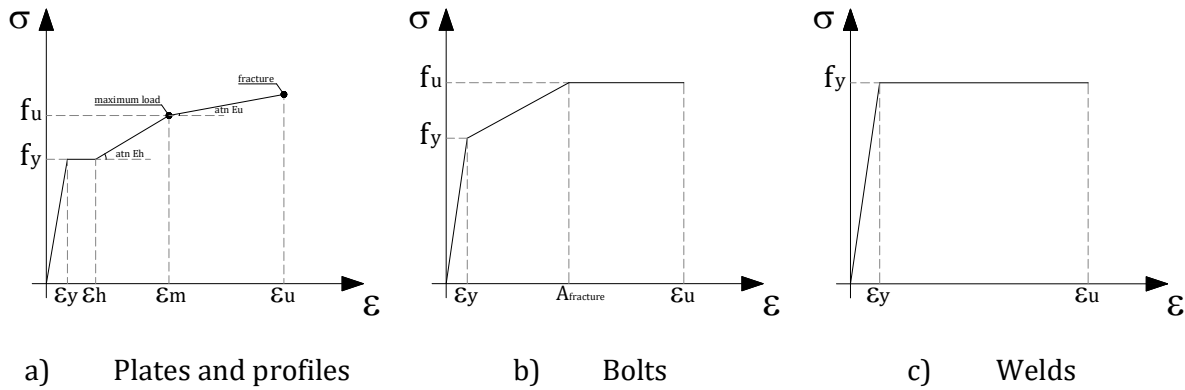


**Figure 8:** Material constitutive laws

320

321 The welds have modelled by means of a bilinear elastic-perfectly plastic law (Fig. 8c) with  
 322 yield strength and ultimate strain defined according to [31].

323 Regarding the value of the yield strength of all the components, consistently with the design  
 324 approach which accounts the influence of random material variability considering the average  
 325 yield strength of the beam flanges, the average value of the yield strength has been adopted for  
 326 the beam component, while for all others components the nominal characteristic value has been  
 327 assumed. This assumption is consistent with the proposed design procedure and with  
 328 ANSI/AISC 358-10 recommendations for prequalified connections for seismic applications  
 329 [32].

330 All the *interactions* between the different elements have been defined using the surface-to-  
 331 surface contact formulation with finite sliding. In particular, the following interactions have  
 332 been defined (Fig. 9): between the end-plate and the column flange, between the bolt head and  
 333 the end-plate, between the bolt shank and the plate hole, between the bolt shank and the  
 334 column flange hole, between the end-plate and the beam end. In the normal direction a “hard  
 335 contact” has been used, while in the tangential direction a friction coefficient equal to 0.20 has  
 336 been adopted.



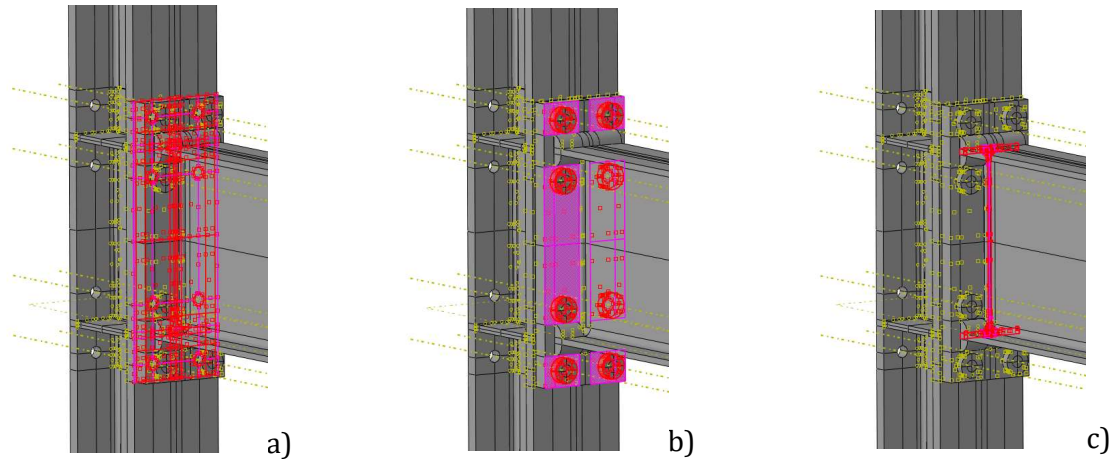


**Figure 9:** Definition of the contacts: a) end-plate/column flange;  
b) bolt head/end-plate; c) end-plate/beam end.

337

338 Where there was the need to link the rigid kinematic mechanisms of the section to those of  
339 a point externally restrained, the constraints have been modelled by introducing at the end of  
340 the section of the members a central node and "coupling internal constraints" (Fig. 10a).

341 In order to simulate the application of an axial force, at the top of the column an external  
342 pressure equal to 30% of the yield strength of the material has been applied (Fig. 10b).

343 Regarding the *finite element type*, in order to reduce the computational efforts, eight-node  
344 brick elements with reduced integration and first order approximation (C3D8R) have been  
345 adopted. The end part of the beam close to the column where local buckling phenomena are  
346 expected, for a length equal to 2.5 times the beam height, has been modelled with non linear  
347 eight-node brick elements with full integration (C3D8). Such elements, as also reported in [32],  
348 are particularly accurate for analysis where buckling effects are significant.

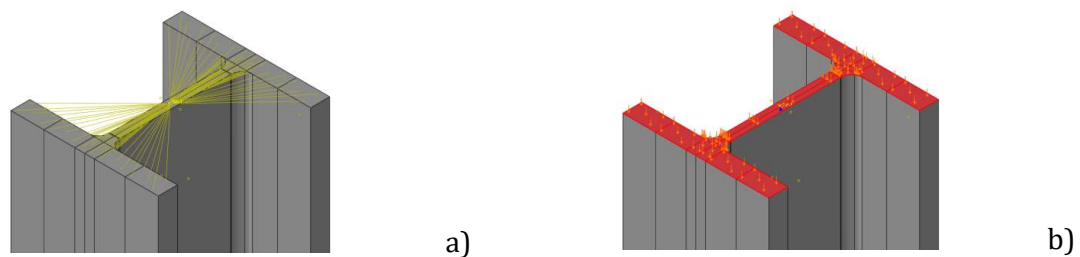


**Figure 10:** a) Coupling internal constrains; b) application of external pressure

349

350 Preliminarily, a sensitivity analysis has been performed in order to determine the *mesh*  
351 *dimension*. The parameters that could influence the results are the number of the elements in  
352 the thickness of the plates, the dimension of the mesh of the bolts and the dimension of the  
353 elements where the local buckling is expected. In order to obtain accurate results, the following

354 “meshing” procedure has been applied: where local buckling is expected the maximum  
 355 dimension of the elements has been taken as 20 mm, the plates with elements whose dimension  
 356 is at least 30 mm and with 2 elements in the thickness, the bolts have been divided using  
 357 elements with minimum dimension equal to 6 mm with a deviation factor equal to 0.1.  
 358 In addition, *geometrical imperfections* have been introduced according to the requirements of  
 359 EN10034 [35], by using a distorted shape of the joint similar to the 1<sup>st</sup> buckling mode  
 360 preliminarily evaluated by means of an elastic buckling analysis. The calibration of the  
 361 distortion of the model has been performed based on the maximum value of the angular  
 362 distortion of the flanges of steel profiles given by EN 1090-2 [36]. The model finalized to the  
 363 execution of the “linear buckling analysis” is depicted in Fig. 11.

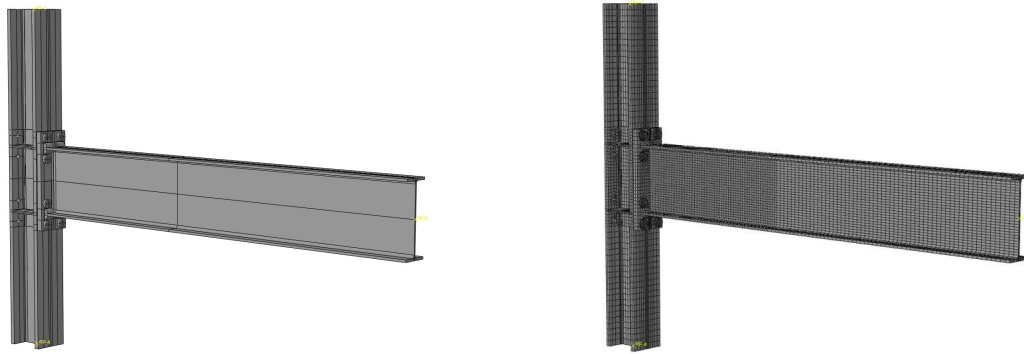


**Figure 11: ABAQUS Model**

364  
 365 The results of the buckling analyses are reported in Fig. 12 representing the first four  
 366 buckling modes. In particular, because of the application of the load downwards, the first and  
 367 the third buckling mode involve the combined buckling of the bottom flange and the  
 368 compressed part of the web. Similarly, the second and the fourth mode provide the buckling of  
 369 the upper flange of the profile when the load is applied upward. Therefore, as the analyses  
 370 developed in this paper are referred to monotonic downward loading conditions, an  
 371 imperfection pattern proportional to first buckling mode has been introduced.

372 Following this approach, the proportionality coefficient  $k_{1^{st}mode}$  for scaling the "buckling  
 373 eigenmode" has been determined as the ratio between the 80% [33] of the maximum  
 374 manufacturing tolerance (equal to 2% of the width of the flange [34]) and the sum of the beam  
 375 flange tip displacements  $\delta_f$  in the buckled configuration:

$$k_{1^{st}mode} = \frac{0.8 \times 0.02 \times b_f}{2 \times \delta_f} \quad (20)$$

376 According to the design criteria adopted, it is expected that plastic deformations are mainly  
 377 located at the beam end. Conversely, the connection components are expected to be subjected  
 378 to very limited yielding. In fact, it should be noted that, even if the joints have been designed to  
 379 attain full strength, limited yielding of joint components has to be expected because the  
 380 formulas used for design, as suggested by Eurocode 3, are based on the definition of design  
 381 plastic resistances rather than on elastic design resistances.  
 382

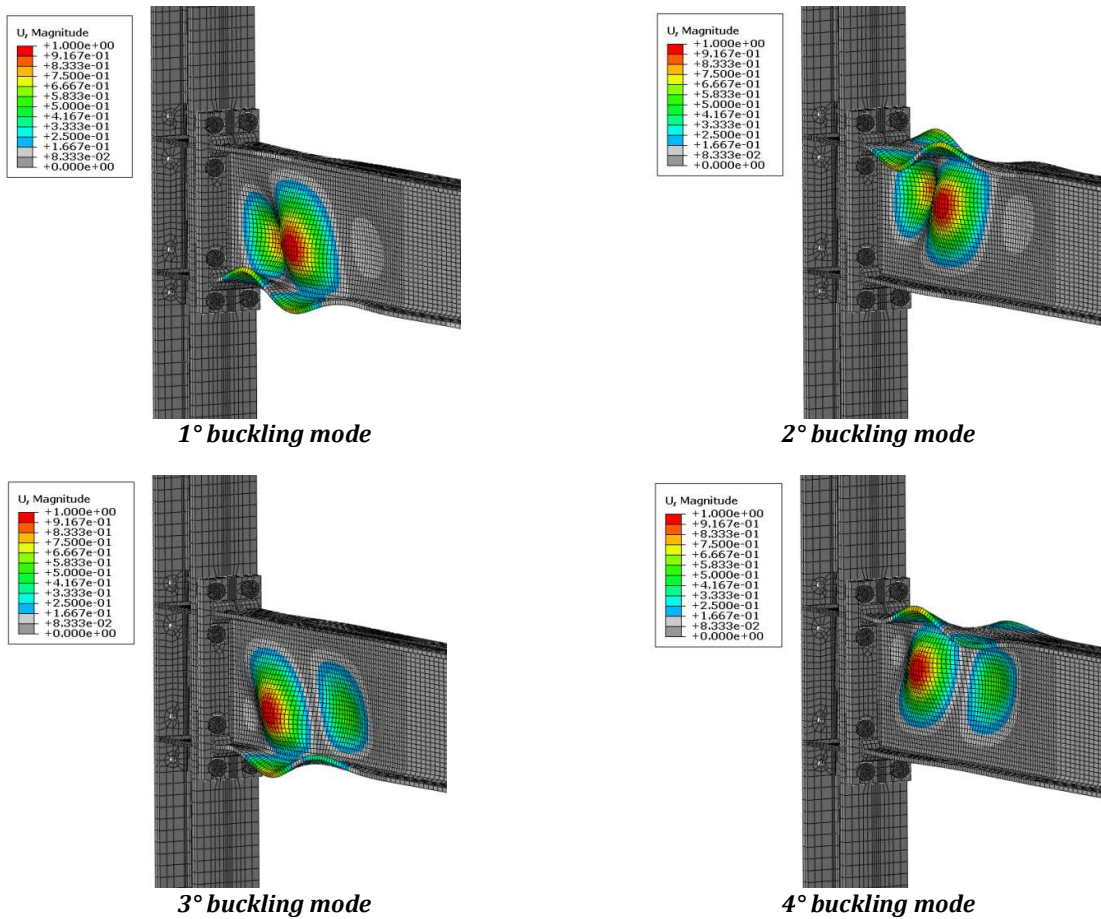
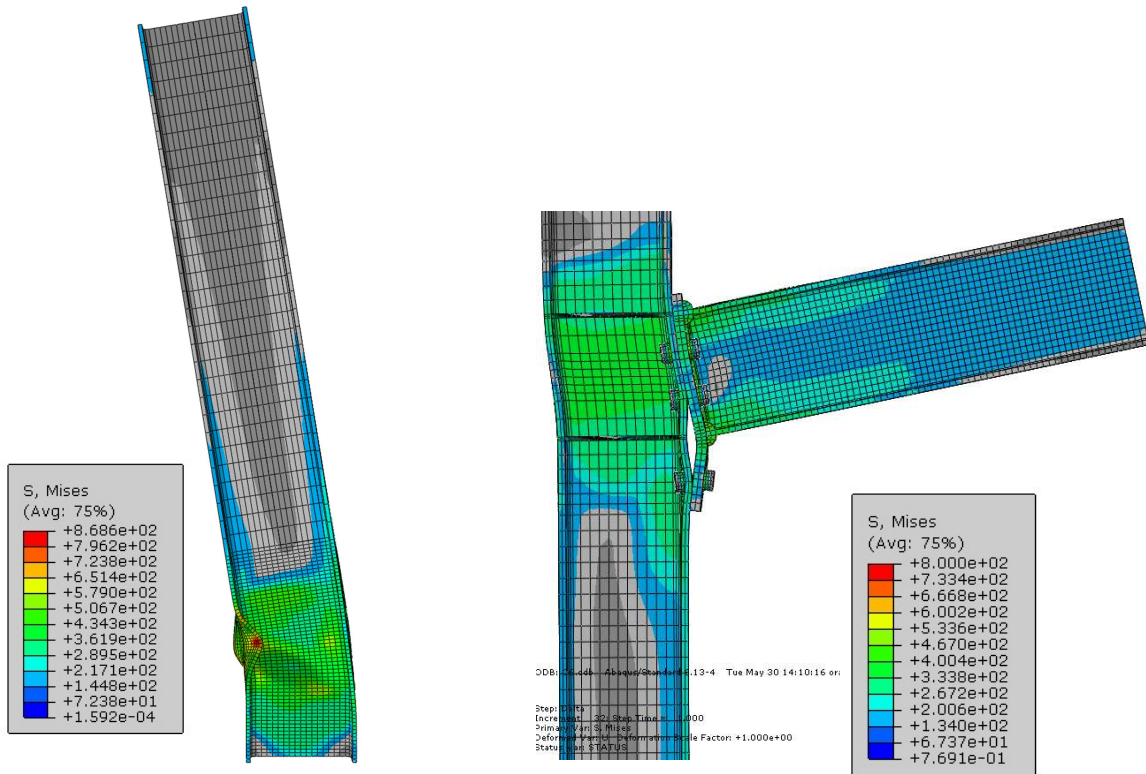


**Figure 12:** buckling modes of beam-to-column joints

383  
 384 The finite element model has been validated through comparison with some experimental  
 385 tests collected from technical literature. Specimens from two different experimental campaigns  
 386 have been considered: a set of tests on full-strength connections described in [37] and a group  
 387 of tests on partial-strength extended end-plate connections reported in [38]. The first group of  
 388 data regards cases where the plastic engagement involves the beam end only and it is used to  
 389 check the model accuracy when the moment-rotation response of the beam-joint system is  
 390 governed by the local buckling of the beam flange in compression. Conversely, the second group

391 of data regards partial strength connections in which several joint components undergo plastic  
 392 deformations. These data are used to check whether or not the FE model is able to reproduce  
 393 accurately the response of the joint.



a) Simulation of the test with IPE 300 [37]

b) Simulation of test C6 [38]

**Figure 13:** Examples of the developed validation FE models

394  
 395 In particular, among the first group of specimens [37], two cases have been selected, one  
 396 regarding a connection fastening an IPE 300 beam, another regarding an HEB 240 profile, both  
 397 made of S275 steel. These tests are non-uniform bending tests carried out under monotonic  
 398 loading conditions. Conversely, among the second group of specimens [38] four specimens  
 399 concerning external beam-to-column joints have been selected, namely those identified in the  
 400 original manuscript [38] as C5, C6, C7 and C8. They concern extended end-plate joints fastening  
 401 rather shallow beams (UB 25.4) to columns with a relatively thin flange (UC 46.2). In these tests,  
 402 the connection and the members are made of an Australian steel grade with nominal yield  
 403 stress equal to 250 MPa and M20 or M16 bolts made up of a steel grade equivalent to the  
 404 European 8.8 class. The connections are realized with a typology similar to that considered in  
 405 this paper, namely with extended end-plate and two internal bolt rows. Case by case, the plates  
 406 have thickness equal to 16 or 20 mm. The results of the validation study are summarized in

407 Figs.13-15 and they evidence the good agreement between FE models and tests in all the  
 408 considered cases. As it is possible to verify easily from the moment-rotation diagrams, the  
 409 model demonstrates to be able to follow with high accuracy the experimental results during the  
 410 whole loading process, simulating accurately both the initial strain-hardening and the softening  
 411 branch arising after the development of local buckling phenomena.

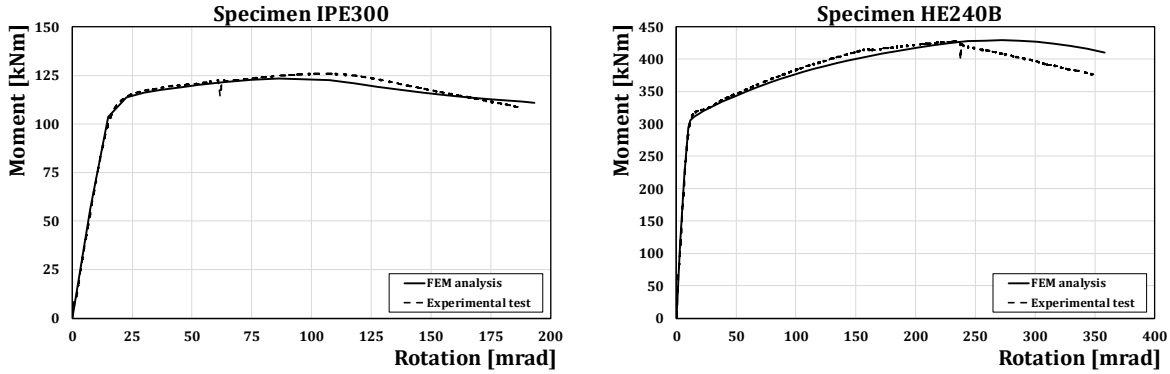


**Figure 14:** Comparison between experimental results [37] and finite element simulation

412 In a similar way, the FE model proves to be able to simulate accurately the moment-rotation  
 413 response of extended end-plate connections (cases C5-C8) when the joint components are  
 414 engaged in plastic range (Fig.15).

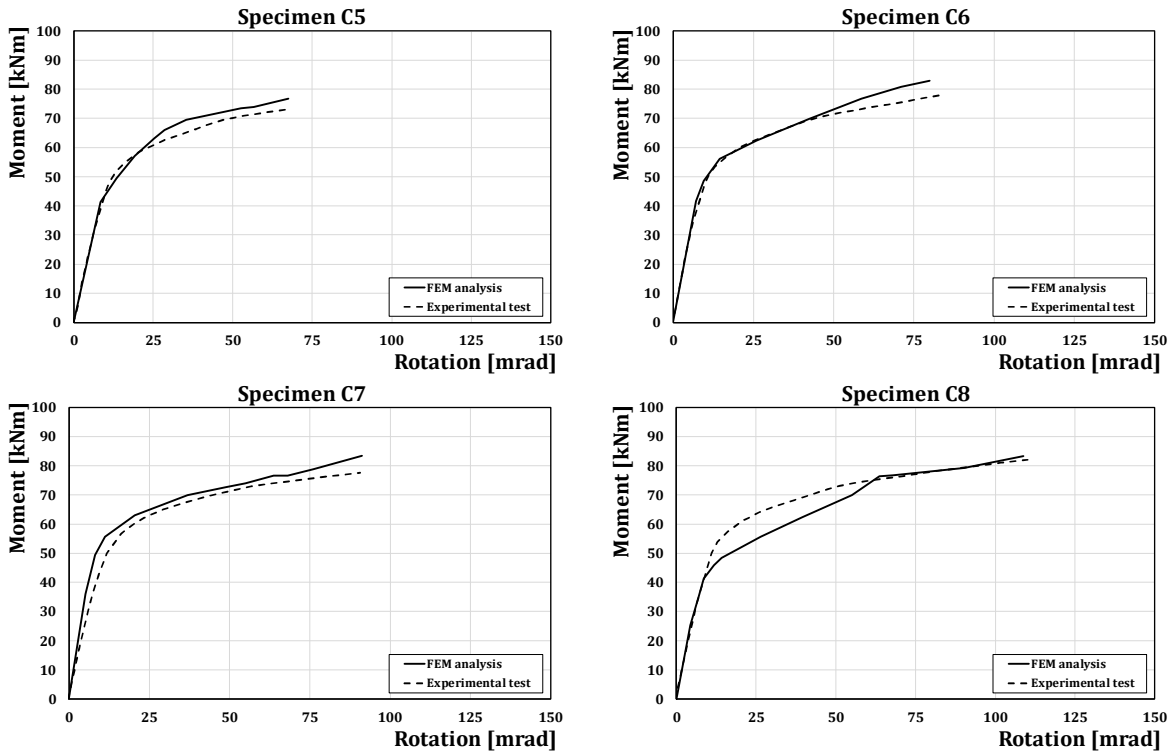


**Figure 15:** Comparison between experimental results [38] and finite element simulation

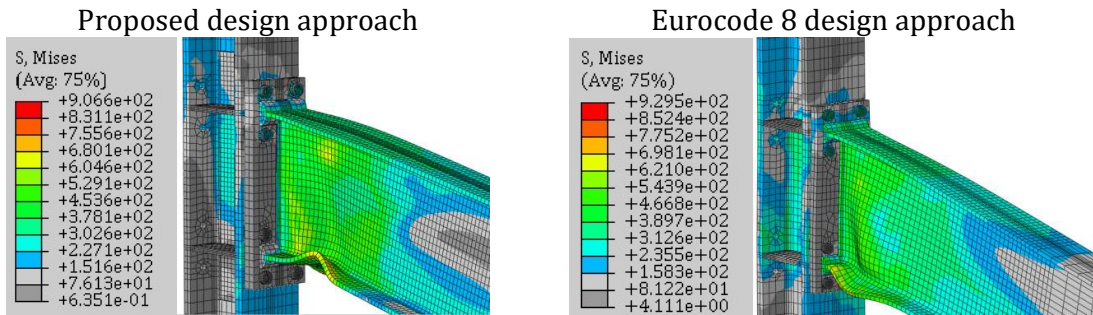


415 In particular, in the four considered cases the components mainly engaged in plastic range  
 416 are the end-plate and the column flange in bending, the shear panel and the bolts in tension and  
 417 shear. Some minor yielding of the beam end also occurs in all the considered cases.

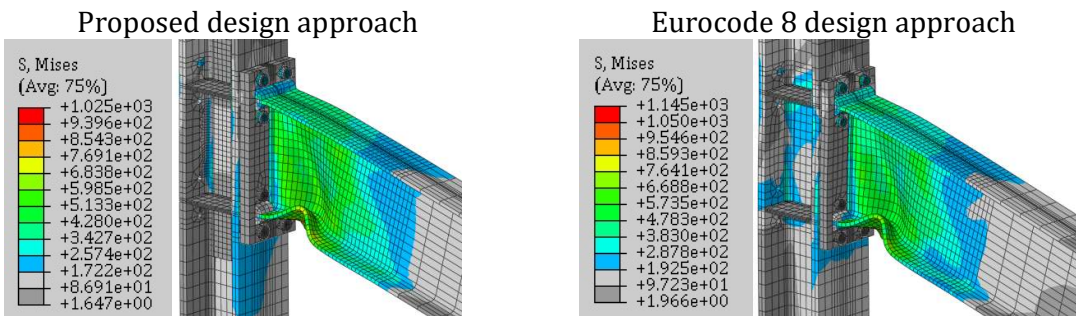
418 **5. RESULTS OF FINITE ELEMENT SIMULATIONS**

419 From the overall point of view, as expected, FE analyses showed in almost all the cases the  
 420 concentration of the plastic deformations at the beam end where the plastic hinge,  
 421 characterized by the development of plastic local buckling of the compressed beam flange and  
 422 out-of-plane buckling of the web, occurred (Fig. 16).

**STUDY CASE A: IPE 600 BEAM – HEM 320 COLUMN**



**STUDY CASE B: IPE 450 BEAM – HEM 260 COLUMN**



**STUDY CASE B: IPE 220 BEAM – HEM 200 COLUMN**

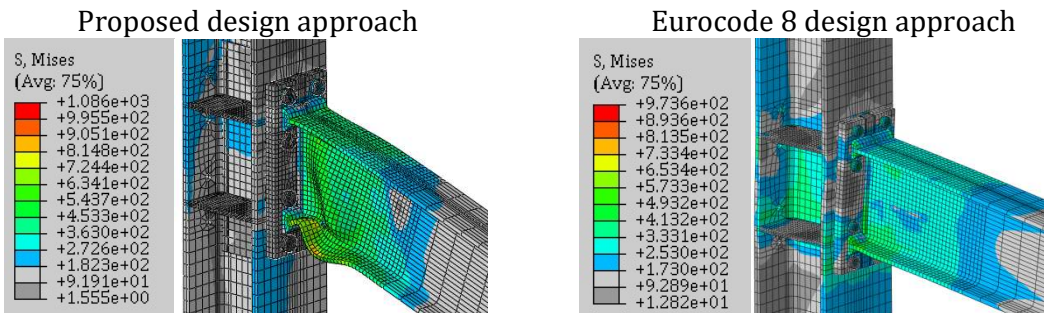


**Figure 16:** Ultimate behaviour of the analysed joints ( Von Mises stresses)

423 The moment-rotation curves of the beam-joint system for all the analysed cases are  
 424 represented in Figs. 17-19. The curves have been obtained, in all cases, by multiplying the force  
 425 applied at the end of the cantilever for  $L_t$  (Fig.6) and dividing the displacement evaluated in the  
 426 same point for the same length.

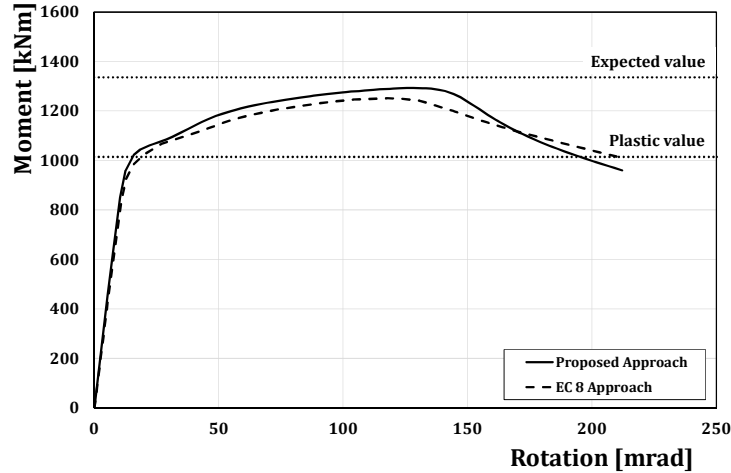


**Figure 17:** Moment-rotation curves (case A)

427  
 428 The curves reported in in Fig.17 are referred to study case A. As expected, after the initial  
 429 linear behaviour, at the attainment of the plastic resistance of the section, they provide a non-  
 430 linear response characterized by the increase of the bending moment, due to the material  
 431 strain-hardening which continues up to the attainment of the local buckling of the beam  
 432 compressed flange. The achievement of the maximum bending moment corresponds to the  
 433 complete development of local buckling. The following softening branch is due to the post-  
 434 buckling behaviour. In the two cases (EC8 and proposed procedure), as it is possible to check  
 435 easily from the figure, the values are very similar and, in particular, equal to 1293 kNm  
 436 (proposed approach) and 1251 kNm (EC8). These values are a little bit lower than the design  
 437 value, evaluated at the column flange level, equal to 1336 kNm. Such scatter, with respect to the  
 438 design value, is very low being less than 7%. It is mainly related to the accuracy of the empirical  
 439 relationship (1) for evaluating  $\gamma_{ov.sh} = s$ .

440 With reference to the case study B, the shape of the moment-rotation curve is analogous to  
 441 the previous case and the values of the moment corresponding to the complete development of  
 442 local buckling of the beam flange are equal to 662 kNm and 666 kNm in case of the joint  
 443 designed according to the proposed approach and to Eurocode 8, respectively. These values of  
 444 the bending moment are practically equal to the design value (663 kNm) confirming the  
 445 accuracy of the formulations used to predict the overstrength factor  $s$  (Fig. 18).

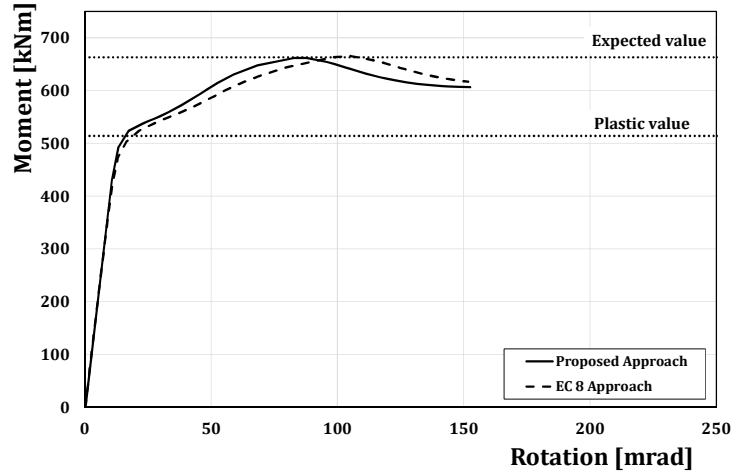


**Figure 18: Moment-rotation curves (case B)**

446

447 Similarly, in the study case C (Fig. 19) the local buckling is achieved in correspondence of a  
 448 bending moment equal to 115 kNm and 113 kNm, respectively, in case of the joint designed  
 449 according to the proposed approach and to Eurocode 8. These values are slightly lower (about  
 450 7% and 8%, respectively) than the design value (equal to 123 kNm). In this case, regarding the  
 451 ultimate rotation, it is useful to underline that the joint designed according to Eurocode 8,  
 452 because of an abrupt drop of the flexural resistance, shows a rotation supply (131 mrad) less  
 453 than the one of the joint designed according to the capacity design criteria proposed.

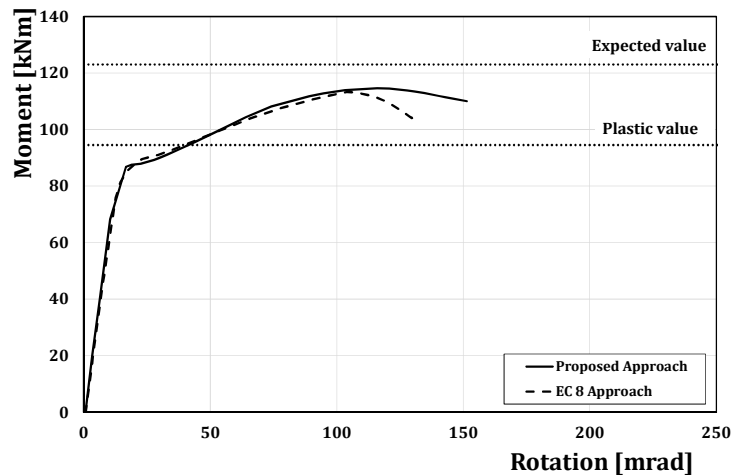


**Figure 19: Moment-rotation curves (case C)**

454

455 This difference is due to the brittle failure of the bolts connecting the end-plate to the column  
 456 flange.

457 As a conclusion, the comparison between the moment-rotation curves of the joints designed  
 458 according to the capacity design criteria herein proposed with those designed according to the



459 EC8 provisions, shows that the differences can be very important, especially concerning the  
460 failure mode, in those cases where EC8 underestimation of the amount of strain-hardening  
461 leads to the bolt failure (case C), undermining significantly the rotation capacity of the beam-  
462 joint system. Even though such brittle behaviour is out of the design philosophy of EC8, it has  
463 been shown that it can actually occur because of the actual overstrength due to the strain  
464 hardening of the material of the connected member, which can be significantly underestimated  
465 by the 1.10 factor adopted by EC8 (as reported in the 4<sup>th</sup> column of Table 3). It is important to  
466 underline that such brittle failure of the bolts may happen even if they are usually oversized  
467 adopting a partial safety factor equal to 1.25, according to EC3.

468 In any case, due to the fact that the EC8 procedure for connections is not completely  
469 rationally addressed, aside from the possible activation of undesired failure modes, in many  
470 cases, it also happens that the plastic engagement of the joint components is significant. This  
471 means that, in case of severe seismic events, the repair of many parts of the connection has to  
472 be accounted for. Conversely, the beam overstrength is more rationally considered by the use  
473 of the capacity design criteria proposed, so that all the joint components are sized for actions  
474 assuring a negligible plastic engagement.

475 In order to quantify the damage of the joints' components, a damage parameter defined as  
476 the ratio between the equivalent plastic deformation (PEEQ) evaluated at the achievement of  
477 the rotational capacity of the beam-joint system and the elastic deformation has been  
478 considered. To this scope, all the components have been isolated and the corresponding  
479 deformation maps have been tracked in order to determine the value of the equivalent plastic  
480 deformation summarized, as summarized in the Tab. 4.

481 With reference to the case study A (IPE 600 beam and HEM 320 column), the results  
482 provided in Tab. 4 point out that the level of yielding occurring in the connection components  
483 is very limited when the beam-to-column joint is designed according to the criteria herein  
484 proposed, achieving a maximum value of 5.57 in the welds; conversely, the use of Eurocode 8  
485 design criteria leads to a normalised PEEQ equal to 63.44 in the bolts and 38.46 in the welds.

486 Even in the study case B (IPE 450 beam and HEM 260 column), the maximum normalized  
487 PEEQ occurs in the welds and is equal to 5.53 for the design procedure proposed while, in case  
488 of Eurocode 8, yielding leads to maximum values of normalised PEEQs equal to 23.82 and 21.49  
489 in the bolts and in the welds, respectively.

490

**Table 4** - Damage to joint components expressed as PEEQ and NPEEQ ( $NPEEQ=PEEQ/\epsilon_y$ )

---

	STUDY CASE A				STUDY CASE B				STUDY CASE C			
	PROPOSED		EUROCODE 8		PROPOSED		EUROCODE 8		PROPOSED		EUROCODE 8	
	PEEQ	NPEEQ	PEEQ	NPEEQ	PEEQ	NPEEQ	PEEQ	NPEEQ	PEEQ	NPEEQ	PEEQ	NPEEQ
<b>Beam</b>	0.3577	319.65	0.3577	319.65	0.8000	714.89	0.9600	857.87	0.9665	863.68	0.1902	169.97
<b>Welds</b>	0.0101	<b>5.57</b>	0.0696	<b>38.46</b>	0.0100	<b>5.53</b>	0.0431	<b>23.82</b>	0.0756	<b>41.78</b>	0.0540	<b>29.84</b>
<b>End-Plate</b>	0.0016	1.25	0.0205	15.68	0.0070	5.35	0.0180	13.75	0.0016	1.22	0.0231	17.64
<b>Column</b>	0.0062	3.65	0.0260	15.35	0.0061	3.61	0.0270	15.97	0.0041	2.43	0.0370	<b>21.89</b>
<b>Supplementary plate</b>	0.0007	0.43	-	-	0.0010	0.59	-	-	0.0016	0.95	-	-
<b>Bolts</b>	0.0177	4.12	0.2719	<b>63.44</b>	0.0116	2.71	0.0921	<b>21.49</b>	0.0012	0.28	0.5053	<b>117.90</b>
<b>Continuity plate</b>	0.0000	0.00	0.0000	0.00	0.0000	0.00	0.0000	0.00	0.0000	0.00	0.0037	2.83

491

492 Finally, in study case C (IPE 220 beam and HEM 200 column), the maximum normalized  
493 PEEQs in the joint components occurs in the welds and is equal to 41.78 in the case of the design  
494 procedure herein proposed while, in case of Eurocode 8, it occurs in the bolts in tension and is  
495 equal to 117.90. Also in this case, damage is highly concentrated at the end of the connected  
496 beam even though the bolts achieve their ultimate capacity in case of the joint designed  
497 according to Eurocode 8.

498 It is important to point out that, even though these PEEQ values have been derived with  
499 reference to monotonic loading conditions, they give an important information about the strain  
500 concentrations occurring in the joint components. These concentrations are of paramount  
501 importance as soon as cyclic loading conditions are considered revealing the probable failure  
502 mode.

## 503 6. CONCLUSIONS

504 In this paper, rigorous capacity design criteria have been suggested to assure the  
505 development of full-strength full-ductility behaviour of beam-to-column joints. The criteria  
506 suggested have been applied and validated by means of FE simulations with reference to  
507 unstiffened extended end-plate connections. In particular, three different external beam-to-  
508 column joints have been designed, according to both the criteria proposed and to Eurocode 8,  
509 and their performances have been compared. The validation of the design criteria has been  
510 made by means of three-dimensional finite element analyses, carried out by ABAQUS 6.13  
511 software.

512 The results obtained, on one hand, have confirmed the accuracy of the design approach and,  
513 on the other hand, have pointed out some criticisms of EC8 design criteria. In fact, EC8  
514 provisions do not rationally account for the overstrength due to the beam strain-hardening. In  
515 particular, in some cases, the underestimation of the overstrength due to strain hardening is

516 not compensated by the partial safety factor commonly applied in bolt design, thus leading to  
517 the brittle failure of the bolts. For the same reason, some joint components are significantly  
518 engaged in plastic range when EC8 design criteria are applied so that the resulting behaviour is  
519 characterized by a significant sharing of yielding between the connected beam end and such  
520 joint components.

521 The effectiveness of the design criteria herein proposed has been demonstrated comparing  
522 the damage level of the joints' components. The results obtained shows that, in case of  
523 connections designed according to the criteria proposed, the damage is conspicuously  
524 concentrated at the end of the beam which constitutes the main dissipative zone while all the  
525 connection's elements practically remain elastic, or only with very limited yielding. Conversely,  
526 in case of joints designed according to Eurocode 8, the joint components are significantly  
527 engaged in plastic range achieving high strain levels, certainly beyond the yield limit. The  
528 developed analyses have demonstrated that following EC8 design procedure, the welds may be  
529 engaged in plastic range with deformations up to 38.46 times the yield strain and, in a similar  
530 way, the bolts may fail or, in general, undergo severe damages.

## 531 ANNEX A: WORKED DESIGN EXAMPLE

532 Seismic design of beam-to-column joints needs the knowledge of the gravity loads acting on  
533 the beams in the seismic load combination, the beam and column sections and the material  
534 properties. The design is aimed to the evaluation of the required bolt diameter, throat thickness  
535 of fillet welds, end-plate thickness, continuity plate thickness and, if needed, thickness of  
536 supplementary web plates. Many relationships are needed to develop all the design steps.  
537 Therefore, in order to clarify the proposed procedure, a worked design example is herein  
538 shown in detail, with reference to the external joint corresponding to study case A, whose input  
539 data are given in Table 2.

540 **Step 1 - Evaluation of the average ultimate moment which the fully yielded and strain**  
541 **hardened beam is able to transmit:**

542 The distance between the plastic hinge and the column flange is:

$$s_h = \frac{d_b}{2} = \frac{600}{2} = 300 \text{ mm}$$

543 The clear length of the beam is  $L_n = 9000 - 359 = 8641 \text{ mm}$  and the distance between the plastic  
544 hinges is  $L_h = L_n - 2s_h = 8641 - 600 = 8041 \text{ mm}$ .

545 The nominal plastic moment of the beam (steel grade S235) is equal to  $M_{b,p} = 786 \text{ kNm}$ .

546 Considering the beam flange thickness, the overstrength coefficient  $\gamma_{ov.rm}$  accounting for the  
547 random variability of the material is given by (see Table 1):

$$\gamma_{ov.rm} = \frac{f_{ym.bf}}{f_{y.b}} = \frac{f_0 - \beta t_{bf}}{f_{y.b}} = \frac{313.4 - 2.254 \times 19}{235} = \frac{270.57}{235} = 1.15$$

548 The average value of the yield stress of the web is equal to:

$$f_{ym.bw} = f_0 - \beta t_{bw} = 313.4 - 2.254 \times 12 = 286.35 \text{ MPa}$$

549 The normalized slenderness parameters of flange and web are equal to:

$$\bar{\lambda}_f = \frac{b_{bf}}{2 t_{bf}} \sqrt{\frac{f_{ym.bf}}{E}} = \frac{220}{2 \cdot 19} \sqrt{\frac{270.57}{210000}} = 0.208$$

$$\bar{\lambda}_w = \frac{d_{bw}}{2 t_{bw}} \sqrt{\frac{f_{ym.w}}{E}} = \frac{562}{2 \cdot 12} \sqrt{\frac{286.35}{210000}} = 0.865$$

550 The beam shear length is equal to  $L_e = L_h/2 = 8041/2 = 4020.5 \text{ mm}$ .

551 The overstrength coefficient accounting for the influence of strain hardening is:

$$Y_{ov.sh} = \frac{1}{0.5463 + 1.6325 \cdot 0.208^2 + 0.0621 \cdot 0.865^2 - 0.6021 \frac{220}{4020.5} + 0.0015 \cdot 37.5 + 0.0078 \cdot 12.3} = 1.28$$

552 Therefore, the average value of the ultimate moment  $M_{b,u}$  which can be transmitted by the  
553 fully yielded and strain-hardened beam is given by:

$$M_{b,u} = 1.15 \cdot 1.28 \cdot 1.05 \cdot 786 \cong 1214 \text{ kNm}$$

554 With reference to the external joint, the value of the shear action at the plastic hinge axis in  
555 the ultimate condition is equal to:

$$V_{bu} = \frac{q L_h}{2} + \frac{n_F F_d}{2} + \frac{2 M_{bu}}{L_h} = \frac{1.25 \cdot 8.041}{2} + \frac{3 \cdot 65.00}{2} + \frac{2 \cdot 1214}{8.041} \cong 404.6 \text{ kN}$$

556

557 **Step 2 - Calculation of bending moment and shear action at the column flange and**  
558 **evaluation of compression force and tensile force to be transmitted at the beam flanges'**  
559 **levels:**

560 The flexural and shear action, respectively  $M_{cf}$  and  $V_{cf}$ , at the column flange are given by:

$$M_{cf} = M_{bu} + V_{bu} \cdot s_h + \frac{q s_h^2}{2} = 1214 + 404.6 \cdot 0.3 + \frac{1.25 \cdot 0.3^2}{2} \cong 1336 \text{ kNm}$$

$$V_{cf} = 404.6 + 1.25 \cdot 0.30 \cong 405 \text{ kN}$$

561 Consequently, the compression/tensile force to be transmitted at the beam flanges' level is  
562 obtained as:

$$T_u = C_u = \frac{M_{cf}}{d_b - t_{bf}} = \frac{1336000}{600 - 19} \cong 2299 \text{ kN}$$

563

564 **Step 3 - Design of the bolt diameter:**

565 For the design of the diameter of the bolts in tension side the following actions have to be  
566 considered:

$$F_{t,Ed} = \frac{T_u}{n_b} = \frac{2299}{4} = 574.75 \text{ kN} \quad F_{v,Ed} = \frac{V_{cf}}{2 n_b} = \frac{405}{2 \cdot 4} = 50.6 \text{ kN}$$

567 where  $n_b$  is the number of bolts in tension.

568 It is important to underline that, in the proposed procedure, the ductility criterion proposed  
569 by the Eurocode 3 Part 1-8 (Section 6.2.7.1) [3] is neglected because ductility requirements are  
570 already taken into account by means of capacity design principles.

571 The check under combined shear and tension lead to evaluation of a first value of the  
572 minimum resistant area needed to the bolts. According to Eurocode 3, for 10.9 bolt class:

$$A_{res} \geq \frac{\gamma_{M2}}{f_{tb}} \left( \frac{F_{v,Ed}}{\alpha_v} + \frac{F_{t,Ed}}{1.26} \right)$$

$$= A_{res} \geq \frac{1.25}{1000} \left( \frac{50600}{0.5} + \frac{574750}{1.26} \right) \cong 696.69 \text{ mm}^2$$

573 where  $A_{res}$  is the tensile stress area of the bolt,  $f_{tb}$  is the ultimate resistance of the bolt'  
 574 material,  $F_{t,Ed}$  is the tensile resistance of the bolt,  $F_{v,Ed}$  is the shear resistance,  $\alpha_v$  is a parameter  
 575 equal to 0.6 for bolt class 4.5, 5.6 and 8.8 and equal to 0.5 for 4.8, 5.8 and 10.9 bolt class.

576 According to Eurocode 3, in any case, the resistant area of the bolts has to be greater than  
 577 the value determined considering only the tension action:

$$A_{res} \geq \frac{\gamma_{M2} F_{t,Ed}}{0.9 f_{tb}} = \frac{1.25 \cdot 574750}{0.9 \cdot 1000} \cong 798.26 \text{ mm}^2$$

578 Consequently, bolts M36 have been chosen.

#### 579 **Step 4 - Design of the welds:**

580 According to Eurocode 3, the design of the welds has been carried out considering the throat  
 581 thickness of the fillet weld in its actual position.

582 With reference to the welds connecting the flange beam to the end-plate, the length of the both  
 583 internal and external fillets has been assumed as:

$$l_f = b_{bf} - 2 \cdot r_b - t_{bw} = 220 - 2 \cdot 24 - 12 = 160 \text{ mm}$$

584 in which  $b_{bf}$  is the beam width,  $r_b$  is the root radius and  $t_{bw}$  is the beam web thickness.

585 Therefore the required throat thickness of the weld is:

$$a_f \geq \frac{T_u}{\sqrt{2} \cdot l_f} \frac{\beta_w \gamma_{M2}}{f_{tk}} = \frac{2299000}{160\sqrt{2}} \frac{0.80 \cdot 1.25}{360} = 28.23 \text{ mm} \rightarrow a_f = 29 \text{ mm}$$

586 where  $\beta_w$  is a correlation factor given by EC3 [3].

587 The welds connecting the web beam and the end-plate have to be able to transmit the shear  
 588 action  $V_{cf}$  and the ultimate flexural action  $M_{w,u}$  that the web flange transmits:

$$M_{w,u} = \gamma_{ov.rm} \cdot \gamma_{ov.sh} \cdot \gamma_{M0} \cdot M_{w,p} = 1.15 \cdot 1.28 \cdot 1.05 \cdot 212.07 \cong 327.77 \text{ kNm}$$

589 The length of the fillets is:

$$l_w = d_{bw} - 2 r_b = 562 - 2 \cdot 24 = 514 \text{ mm}$$

590 where  $d_{bw}$  is the height of the beam web. The thickness results to be:

$$a_w \geq \frac{\beta_w \gamma_{M2}}{f_{tk}} \frac{1}{l_w} \sqrt{\frac{8 M_{w,u}^2}{l_w^2} + \frac{3}{4} V_{cf}^2} = \frac{0.8 \cdot 1.25}{360} \frac{1}{514} \sqrt{\frac{8 (327.77 \cdot 10^6)^2}{514^2} + \frac{3}{4} (405 \cdot 10^3)^2}$$

$$\cong 9.92 \text{ mm} \rightarrow a_w = 10 \text{ mm}$$

591

592 **Step 5 – Design of the end-plate:**

593 Considering the design criteria already adopted for the bolts, failure mechanism type 3 can  
 594 be excluded. Therefore, only the resistance formulations for mechanism type 1 and mechanism  
 595 type 2 have to be considered to check the equivalent T-stub modelling the end-plate in bending.  
 596 It is assumed that the distance  $m$  between the bolt axis and the plastic hinge located close to the  
 597 beam flange is equal to the minimum technologically compatible,  $m=1.2 d_0$  being  $d_0$  the diameter  
 598 of the bolt hole. In addition, the width of the plate is defined on the basis of the code  
 599 requirements for bolt spacing and of technological conditions.

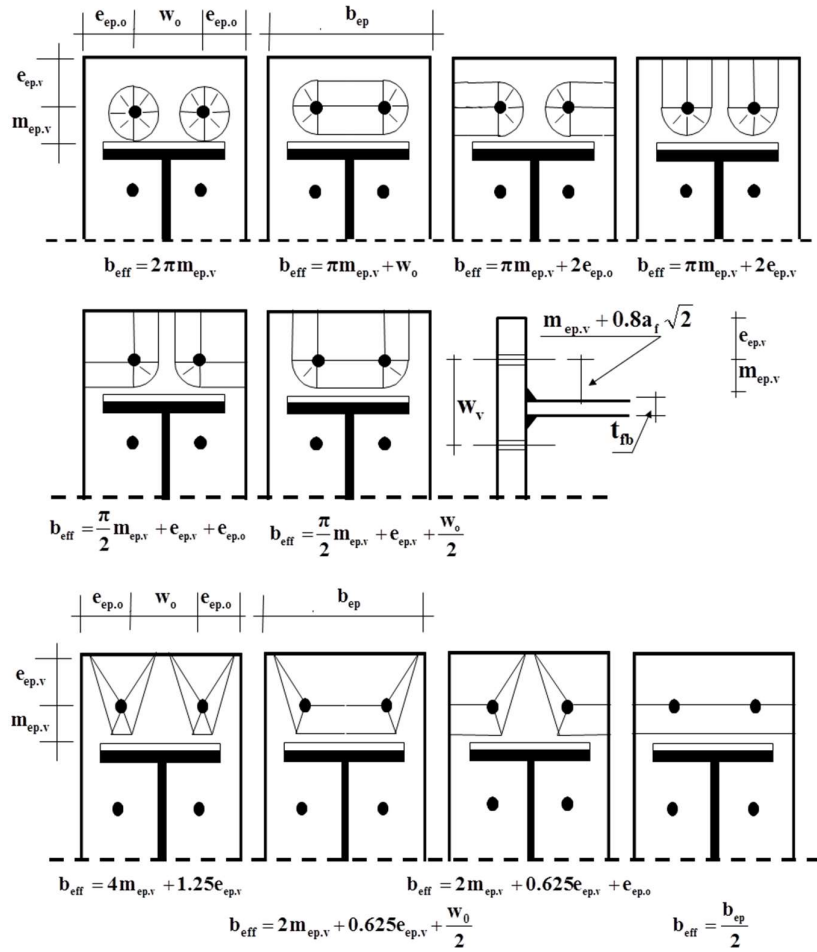


**Figure 17 - Determination of the effective length for a single bolt row on the basis of the possible collapse mechanisms**

600 The horizontal distance between the bolts  $w$  has to satisfy the following limitations:

$$w_{\min} \cong t_{cw} + 2 r_c + 1.8 d_0 = 21 + 2 \cdot 27 + 1.8 \cdot 37.5 = 142.5 \text{ mm}$$

$$w_{\max} = b_{cf} - 2.4 d_0 = 309 - 2.4 \cdot 37.5 = 219 \text{ mm}$$

601 where  $t_{cw}$  is the thickness of the column web,  $r_c$  the root radius of the column,  $d_0$  the hole  
 602 diameter and  $b_{cf}$  the width of the column.

603 According to the above limitations, the bolt spacing is taken equal to  $w_0 = 170 \text{ mm}$ .

604 Regarding the width of the end-plate, it should be greater than:

$$b_{ep} = \max\{w + 2.4 d_0; b_{bf}\} = \max\{170 + 2.4 \cdot 37.5; 220\} = 260 \text{ mm}$$

605 and, anyway, smaller than the width of the column that is equal to 309 mm, consequently the  
 606 width of the end plate is taken equal to 280mm.

607 As a consequence, the horizontal distance between the bolt axis and the edge of the plate  $e_{ep,0}$   
 608 is:

$$e_{ep,0} = \frac{b_{ep} - w_0}{2} = \frac{280 - 170}{2} = 55 \text{ mm}$$

609 For the evaluation of the effective length of the equivalent T-stub, taken  $m_x = e_x = 1.2d_0 =$   
 610  $45 \text{ mm}$ , it results:

$$b_{eff,ep,1} = \min\{2\pi m_x; \pi m_x + w; \pi m_x + 2e_{ep}\} = \min\{282.6; 311.3; 251.3\} = 251.3 \text{ mm}$$

611 which accounts for the circular patterns and:

$$\begin{aligned} b_{eff,ep,2} &= \min\{4m_x + 1.25e_x; e_{ep} + 2m_x + 0.625e_x; 0.5w + 2m_x + 0.625e_x\} = \\ &= \min\{4 \cdot 45 + 1.25 \cdot 45; 45 + 2 \cdot 45 + 0.625 \cdot 45; 0.5 \cdot 170 + 2 \cdot 45 + 0.625 \cdot 45\} = \\ &= \min\{236.25; 173.12; 203.12\} = 203.12 \text{ mm} \end{aligned}$$

612 which accounts for non-circular patterns.

613 Definitely, the effective length of the equivalent T-stub is:

$$b_{eff,ep} = \min\{b_{eff,1}; b_{eff,2}; 0.5 b_{ep}\} = \min\{251.3; 203.12; 0.5 \cdot 280\} = 140 \text{ mm}$$

614 The thickness of the end-plate required to avoid the collapse of the equivalent T-stub according  
 615 to type-1 mechanism is:

$$\begin{aligned} F_{1,Rd} &= 2 \frac{b_{eff} t_{ep}^2 f_{y,ep}}{m \gamma_{M0}} = T_u \rightarrow t_{ep,1} = \sqrt{\frac{m_x T_u \gamma_{M0}}{2 \cdot b_{eff,ep} \cdot f_{y,ep}}} = \sqrt{\frac{45 \cdot 2299000 \cdot 1.05}{2 \cdot 140 \cdot 275}} \\ &\cong 37.56 \text{ mm} \end{aligned}$$

616 Similarly, to avoid the collapse of the equivalent T-stub according to type-2 mechanism the  
 617 required end-plate thickness is:



$$F_{2,Rd} = 2 \frac{\frac{f_{y,ep} b_{eff} t_{ep}^2}{2} + 2 F_{t,Rd} n}{m + n} = T_u \quad \rightarrow \quad t_{ep,2} = \sqrt{\frac{2 \gamma_{M0}}{b_{eff,ep} f_{y,ep}} \left[ \frac{T_u (m_x + e_x)}{2} - 2 F_{t,Rd} e_x \right]} =$$

$$= \sqrt{\frac{2 \cdot 1.05}{140 \cdot 275} \left[ \frac{2299000 (45 + 45)}{2} - 2 \cdot 588240 \cdot 45 \right]} \cong 52.50 \text{ mm}$$

618 Therefore, the thickness of the end-plate has been assumed equal to 55mm.

619

620 **Step 6 - Check of the resistance of the column web in shear and design of supplementary**  
621 **web plates if needed:**

622 The shear resistant area of the column section is given by:

$$A_{vc} = A - 2 b_{cf} t_{cf} + (t_{cw} + 2r_c)t_{cf} = 31200 - 2 \cdot 309 \cdot 40 + (21 + 2 \cdot 27) \cdot 40$$

$$= 9480 \text{ mm}^2$$

623 The resistance of the column web panel, without continuity and/or supplementary plates, is:

$$V_{wp,Rd} = \frac{0.9 \cdot A_{vc} \cdot f_{y,cw}}{\sqrt{3} \cdot \gamma_{M0}} = \frac{0.9 \cdot 9480 \cdot 355}{\sqrt{3} \cdot 1.05} \cong 1665 \text{ kN}$$

624 Since continuity plates in the both compression and tension zones have been considered, the  
625 plastic shear resistance of the column web panel is incremented by the contribution due to the  
626 resistant mechanism activated by the continuity plates.

627 The plastic moment of the column flange is given by:

$$M_{pl,cf,Rd} = \frac{b_{cf} t_{cf}^2 f_{y,c}}{4 \gamma_{M0}} = \frac{309 \cdot 40^2 \cdot 355}{4 \cdot 1.05} \cong 41.79 \text{ kNm}$$

628 Therefore the contribution due to the additional resistant mechanism activated by the  
629 continuity plates results:

$$V_{wp,add,Rd} = \frac{4 \cdot M_{pl,cf,Rd}}{d_s} = \frac{4 \cdot 41.79}{0.581} = 287.7 \text{ kN}$$

630 where  $d_s$  is the distance between the centrelines of the stiffeners.

631 The total resistance of the column web panel is:

$$V_{wp,Rd,tot} = V_{wp,Rd} + V_{wp,add,Rd} = 1665 + 287.7 \cong 1953 \text{ kN}$$

632 Whereas the shear resistance of the column web panel is lower than the action transmitted by  
633 the beam in its ultimate conditions, supplementary web plates are needed whose width is taken  
634 equal to:

$$b_{s,max} = d_{cw} - 2r_c = 279 - 2 \cdot 27 = 225 \text{ mm}$$

635 According to Eurocode 3, the resistance of the material constituting the supplementary  
636 plates has to be the same of the column; the thickness of the stiffeners results to be:

$$t_s \geq \frac{\sqrt{3} \cdot \gamma_{M0} (T_u - V_{wp,add,Rd})}{0.9 \cdot b_s \cdot f_{y,wc}} - \frac{A_{vc}}{b_s} = \frac{\sqrt{3} \cdot 1.05 \cdot (2299000 - 287700)}{0.9 \cdot 225 \cdot 355} - \frac{9480}{225}$$

$$\cong 9.76 \text{ mm}$$

637 Consequently, it is possible to use a couple of supplementary plates whose thickness is 5 mm  
638 or a single supplementary web plate whose thickness is equal to 10 mm.

639

640 **Step 7 - Check of the resistance of the column web in tension and in compression.**

641 Since continuity plates have been considered in the evaluation of the shear resistance of the  
642 column web panel, their design is required. The transverse stiffeners can be designed according  
643 to two possible approaches. The first approach requires that the action transmitted from the  
644 beam flanges in their ultimate conditions, equal to  $T_u$ , is absorbed relying exclusively on the  
645 tensile/compression resistance of continuity plates, neglecting the resistance of the column  
646 web. The second approach allows the reduction of the thickness of the continuity plates, taking  
647 advantage of the contribution due to the resistance of the column web.

648 In accordance to the latter, the resistance of the column web in compression and the  
649 resistance of the continuity plates have to be determined; the former is given by:

$$F_{cwc,Rd} = b_{eff,cwc} (t_{cw} + t_{s,tot}) \cdot \frac{f_{y,cw}}{\gamma_{M0}} = \frac{546.02 (21 + 10) 355}{1.05} \cong 5723 \text{ kN}$$

650 where  $t_{cw}$  is the thickness of the column web and  $b_{eff,cwc}$  is the effective length of the column  
651 web given by:

$$b_{eff,cwc} = t_{fb} + 2\sqrt{2} a_f + 5(t_{fc} + r_c) + 2 t_{ep} = 19 + 2\sqrt{2} \cdot 29 + 5(40 + 27) + 2 \cdot 40 \cong 546.02 \text{ mm}$$

652 and  $t_{s,tot} = 10 \text{ mm}$  is the thickness of the supplementary web plates.

653 Obviously, if  $F_{cwc,Rd} \geq T_u$  it is possible to evaluate the possibility of omitting the continuity  
654 plates. In such a case, it is necessary to check again the resistance of column web in shear  
655 according to Step 6.

656 Subsequently, the welds have been designed:

$$a_{cp} \geq \frac{\beta_w t_{cp} f_{y,cp}}{\sqrt{2} f_{tk}} = \frac{0.85 \cdot 20 \cdot 275}{\sqrt{2} \cdot 430} \cong 7.68 \text{ mm} \quad \rightarrow \quad a_{cp} = 8 \text{ mm}$$

657

658

659

660 **Step 8 - Check of the resistance of the column flange in bending:**

661 In bolted connections, an equivalent T-stub in tension may be used to model the design  
 662 resistance of the column flange in bending. As highlighted for the end-plate in bending, failure  
 663 mode according to mechanism type-3 can be excluded because of the design criterion adopted  
 664 for the bolts. Therefore, the design resistances for mechanism type-1 and type-2 have to be  
 665 evaluated. In particular, the following equation has to be considered:

$$F_{1,Rd} \geq T_u \quad F_{2,Rd} \geq T_u$$

666 where:

$$F_{1,Rd} = 2 \frac{b_{eff} t_{cf}^2 f_{y,cf}}{m \gamma_{M0}} \quad \text{and} \quad F_{2,Rd} = 2 \frac{\frac{f_{y,cf} b_{eff} t_{cf}^2}{\gamma_{M0}} + 2 F_{t,Rd} n}{m + n}$$

667 in which  $b_{eff}$  is the effective length of the equivalent T-stub corresponding to a single bolt row,  
 668  $t_{cf}$  is the thickness of the column flange,  $m$  is the distance between the bolt line and the plastic  
 669 hinge arising at the T-stub stem,  $n$  is the distance between the bolt line and the end of the plate  
 670 where the contact forces are concentrated and  $f_{y,cf}$  is the yield resistance of the column flange.

671 With reference to Fig. 18a it is possible to define:

$$m_c = \frac{w - t_{wc} - 1.6 r_c}{2} = \frac{170 - 21 - 1.6 \cdot 27}{2} = 52.9 \text{ mm}$$

672 while the horizontal distance between the bolt axis and the edge of the column flange is:

$$e = \frac{b_c - w}{2} = \frac{309 - 170}{2} = 69.5 \text{ mm}$$

673 The vertical distance between the first and second bolt rows is:

$$w_v = 2 (m + 0.8 a_f \sqrt{2} + t_{fb}/2) = 2 (45 + 0.8 \cdot 29 \sqrt{2} + 19/2) = 174.62 \text{ mm}$$

674 In presence of continuity plates whose fillet welds have a throat thickness equal to 8 mm, it  
 675 results:

$$m_2 = \frac{w_v - t_{cp} - 1.6 a_{cp} \sqrt{2}}{2} = \frac{174.62 - 20 - 1.6 \cdot 8 \sqrt{2}}{2} = 68.26 \text{ mm}$$

676 According to Eurocode 3 the effective length, in presence of transverse stiffeners, is given by:

$$b_{eff} = \min\{2\pi m_c; \alpha \cdot m_c\} = \min\{2\pi \cdot 52.9; 5.93 \cdot 52.9\} \cong 313.7 \text{ mm}$$

677 where the parameter  $\alpha$  has been determined considering the geometrical parameters  $\lambda_1$  and  
 678  $\lambda_2$ :

$$\lambda_1 = \frac{m_c}{m_c + e} = \frac{52.9}{52.9 + 69.5} = 0.43$$

$$\lambda_2 = \frac{m_2}{m_c + e} = \frac{68.26}{52.9 + 69.5} = 0.57$$

679 by means the abacus in Fig. 18b:

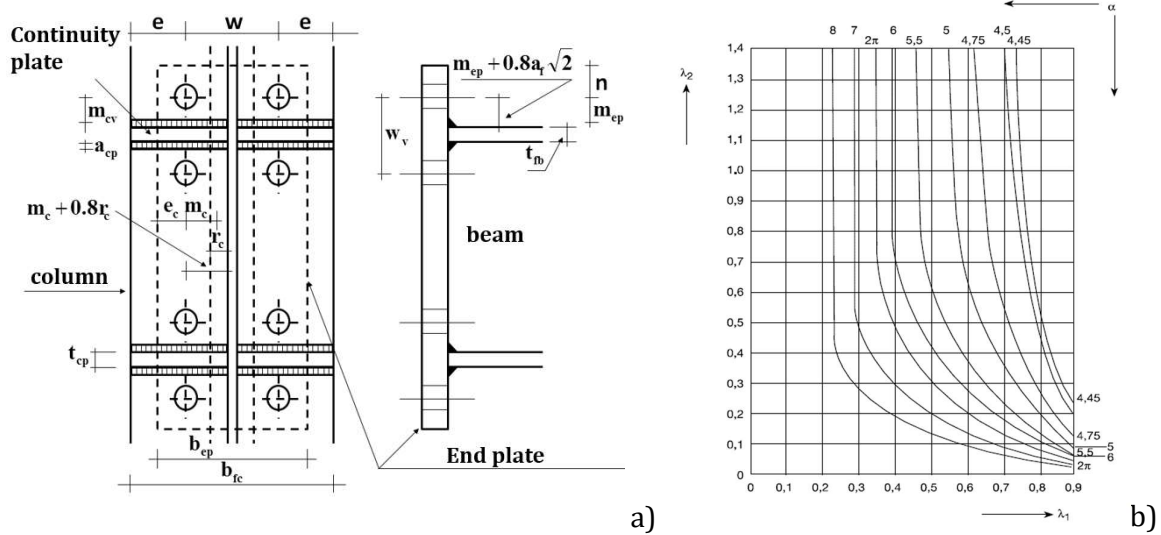


Figure 18: Column flange: a) geometrical properties; b) abacus

680

681 Thereafter, the design resistances for mechanisms type-1 and type-2 are given by:

$$F_{1,Rd} = 2 \frac{f_{y,cf} b_{eff,cfb} t_{cf}^2}{m_c} \frac{1}{\gamma_{M0}} = 2 \frac{355 \cdot 313.7 \cdot 40^2}{52.9} \frac{1}{1.05} \cong 6416 \text{ kN} \geq T_u$$

$$F_{2,Rd} = 2 \frac{f_{y,cf} \frac{b_{eff,cfb} t_{cf}^2}{2} + 2 F_{t,Rd} n}{m_c + n} \frac{1}{\gamma_{M0}} = 2 \frac{355 \frac{313.7 \cdot 40^2}{2} + 2 \cdot 588240 \cdot 55}{52.9 + 55} \frac{1}{1.05} \cong 2715 \text{ kN} \geq T_u$$

682 where  $n = \min\{e; e_{ep}; 1.25m_c\} = \min\{69.5; 55; 1.25 \cdot 52.9\} = 55 \text{ mm}$ .

683 Since the both design resistances are greater than the action  $T_u$ , derived by means of capacity

684 design principles, the check of the column flange in bending is satisfied.

685 **REFERENCES**

- 686 [1] J.P. Jaspart: "Etude de la semi-rigidité des noeuds poutre-colonne et son influence sur la  
687 résistance et la stabilité des ossatures en acier" PhD Thesis, University of Liège, Liège,  
688 1991.
- 689 [2] F. Mazzolani and V. Piluso: "An attempt of codification of semirigidity for seismic  
690 resistant steel structures", Third international workshop on connections in steel  
691 structures, Trent, 28-31 May, 1992.
- 692 [3] CEN (2005): "Eurocode 3: Design of Steel Structures – Part 1-8: Design of Joints", EN  
693 1993-1-8.
- 694 [4] D.B. Moore, F. Wald (ed.): "Design of Structural connections to Eurocode 3 – Frequently  
695 Asked Questions", Building Research Establishment Ltd, Watford, 2003, ISBN 80-01-  
696 02838-0, Project Continuing Education in Structural Connections, No. CZ/00/B/F/PP-  
697 134099, Leonardo Da Vinci, Programme.
- 698 [5] Latour, M. and Rizzano, G., (2013b), "A Theoretical Model for Predicting the Rotational  
699 Capacity of Steel Base Joints", Journal of Constructional Steel Research, 91, pp. 88-99.
- 700 [6] Latour, M., Piluso, V. and Rizzano, G., (2014d), "Rotational Behaviour of Comun Base  
701 Plate Connections: Experimental Analysis and Modelling", Engineering Structures, pp.  
702 14-23.
- 703 [7] Girao Coelho, A. M., Bijlaard, F. & Simoes Da Silva, L., (2004), "Experimental Assessment  
704 of the Ductility of Extended End Plate Connections" Engineering Structures, 26, pp.  
705 1185-1206.
- 706 [8] Beg, D., Zupancic, E. & Vayas, I., (2004), "On the Rotation Capacity of Moment  
707 Connections", Journal of Constructional Steel Research, 60, pp. 601-620.
- 708 [9] Piluso, V., Rizzano, G. (2008), "Experimental analysis and modelling of bolted T-stubs  
709 under cyclic loads", Journal of Constructional Steel Research, Vol. 64, pp. 655-669.
- 710 [10] Iannone, F., Latour, M., Piluso, V. & Rizzano, G., (2011), "Experimental Analysis of Bolted  
711 Steel Beam-to-Column Connections: Component Identification", Journal of Earthquake  
712 Engineering, 15(2), pp. 214-244.
- 713 [11] Latour, M., Piluso, V. and Rizzano, G., (2011a), "Experimental Analysis of Innovative  
714 Dissipative Bolted Double Split Tee Beam-to-Column Connections", Steel Construction,  
715 June, 4(2), pp. 53-64.

- 716 [12] Hu, J., Leon, R. and Park, T., (2012), "Mechanical Models for the Analysis of Bolted T-stub  
717 Connections under Cyclic Loads", *Journal of Constructional Steel Research*, 78, pp. 45-  
718 57.
- 719 [13] Bravo, M. and Herrera, R., (2014) "Performance under cyclic load of built-up T-stubs for  
720 Double T moment connections. *Journal of Constructional Steel Research*, Volume 103,  
721 pp. 117-130.
- 722 [14] C. Faella, V. Piluso and G. Rizzano: "Structural Steel Semirigid Connections", CRC Press,  
723 Boca Raton, Ann Arbor, London, Tokyo. ISBN 0-8493-7433-2, 1999.
- 724 [15] U.Kuhlmann: "Definition of Flange Slenderness Limits on the Basis of Rotation Capacity  
725 Values", *Journal of Constructional Steel Research*, pp. 21-40, 1989.
- 726 [16] B. Kato: "Rotation Capacity of H-section members as determined by local buckling",  
727 *Journal of Construction Steel Research*, 13, 95-109, 1989.
- 728 [17] F.M. Mazzolani and V. Piluso: "Evaluation of the rotation capacity of steel beams and  
729 beam-column", 1st COST C1 Workshop, Strasbourg, 28-30 October, 1992.
- 730 [18] B. Kato: "Rotational Capacity of steel members subject to Local Buckling", *9<sup>th</sup> World  
731 Conference on Earthquake Engineering*, Vol. IV, paper 6-2-3, August 2-9, Tokyo-Kyoto,  
732 1988.
- 733 [19] Y.E. Yee and R.E. Melchers: "Moment-rotation curves for bolted connections", *Journal of  
734 Structural Engineering*, ASCE, Vol. 112, Issue 3, pp. 615-635, 1986.
- 735 [20] B. Kato: "Deformation Capacity of Steel Structures", *Journal of Constructional Steel  
736 Research*, pp. 33-94, N.17, 1990.
- 737 [21] A. Girao Coelho: Characterization of the ductility of bolted extended end plate beam-to-  
738 column steel connections. PhD Thesis: Universidade de Coimbra, 2004.
- 739 [22] CEN, EN 1998-1-1. Eurocode 8: Design of structures for earthquake resistance - Part 1:  
740 General rules, seismic actions and rules for buildings, *European committee for  
741 standardization*, 2005.
- 742 [23] Ministero delle Infrastrutture: "Norme tecniche per le costruzioni", NTC2008, 2008.
- 743 [24] V. Piluso and G. Rizzano: "Random material variability effects on full-strength end-plate  
744 beam-to-column joints", *Journal of constructional steel research*, vol.63, 2007.
- 745 [25] G.L. Tucker and R.M. Bennet: "Reliability Analysis of Partially Restrained Steel  
746 Connections", *Journal of Structural Engineering*, ASCE, Vol. 116, No. 4, April, pp. 1090-  
747 1101, 1990.

- 748 [26] R.M. Bennett and F.S. Najem-Clarke: "Reliability of Bolted Steel Tension Members",  
749 *Journal of Structural Engineering, ASCE*, Vol.113, No. 8, pp. 1865-1872, 1987.
- 750 [27] H. Gervásio, L. Simões da Silva and L. Borges: "Reliability assessment of the post-limit  
751 stiffness and ductility of steel joints", *Third European Conference on Steel Structures*,  
752 Coimbra, 2002, September 19-20, 2002.
- 753 [28] R.Y. Rubinstein: "Simulation and the Monte Carlo method", John Wiley & Sons, 1981.
- 754 [29] J.W. Fisher, T.V. Galambos, G.L. Kulak and M.K. Ravindra: "Load and resistance factor  
755 design criteria for connection", *ASCE annual Convention & Exposition*, Chicago, October  
756 16-20, 1978.
- 757 [30] Gruppo Fontana, Catalogo Tecnico: Prescrizioni Tecniche, 2004.
- 758 [31] BS-EN-ISO 2560. Welding consumables: covered electrodes for manual metal arc  
759 welding of non-alloy and fine grain steels, Classification, 2009.
- 760 [32] ANSI/AISC 358-10, ANSI/AISC 358s1-11: "Prequalified Connections for Special and  
761 Intermediate Steel Moment Frames for Seismic Applications", 2011.
- 762 [33] O.S. Bursi and J.P. Jaspart: "Calibration of a finite Element model for isolated bolted end-  
763 plate steel connections", *Journal of Constructional Steel Research* 44, 224-262,1997.
- 764 [34] CEN, EN 1993-1-5. Eurocode 3: Design of steel structures - Part 1-5: Plated structural  
765 elements, *European committee for standardization*, 2007.
- 766 [35] CEN, EN 10034. Structural steel I and H sections – Tolerances on shape and dimensions,  
767 *European committee for standardization*, 1993.
- 768 [36] CEN, EN 1090-2. Execution of steel structure and aluminium structure: Technical  
769 requirements for steel structures. Annex G: Test to determine slip factor, 2008.
- 770 [37] M. D'Aniello, R. Landolfo, V. Piluso and G. Rizzano: "Ultimate behavior of steel beams  
771 under non-uniform bending", *Journal of Constructional Steel Research*, 78, 144-158,  
772 2012.
- 773 [38] A.K. Aggarwal: "Comparative Tests On Endplate Beam-To-Column Connections", *Journal*  
774 *of Constructional Steel Research*, 30, 151-175,1994.
- 775 [39] A.B. Francavilla, M. Latour, V. Piluso, G. Rizzano, Simplified finite element analysis of  
776 bolted T-stub connection components, *Eng. Struct.* 100 (2015) 656–664.
- 777 [40] A.B. Francavilla, M. Latour, V. Piluso, G. Rizzano, Bolted T-stubs: A refined model for  
778 flange and bolt fracture modes, *Steel Compos. Struct.* 20 (2) (2016) 267–293.

779 [41] C. Chisari, A.B. Francavilla, M. Latour, V. Piluso, G. Rizzano, C. Amadio, Critical issues in  
780 parameter calibration of cyclic models for steel members, Eng. Struct. 132 (2017) 123–  
781 138.